Alma Mater Studiorum – Università di Bologna

DOTTORATO DI RICERCA IN

Scienze Biomediche e Neuromotorie

Ciclo XXXIII

Settore Concorsuale: 05/H1

Settore Scientifico Disciplinare: BIO/16

Cellular signalling and morphological alterations in Autosomal Dominant Leukodystrophy

Presentata da:

Dott.ssa Isabella Rusciano

Supervisore:

Prof. Lucio Ildebrando Cocco

Coordinatore Dottorato:

Prof. Pietro Cortelli

Co-supervisori:

Prof.ssa Lucia Manzoli
Prof.ssa Giulia Ramazzotti
Dott. Stefano Ratti

Esame Finale Anno 2020

Summary

Abstract

Autosomal Dominant Leukodystrophy (ADLD) is a neurodegenerative disorder that affects the central nervous system. It is a rare and late onset lethal progressive disorder without any effective treatment up to date. Genetically it is characterized by Lamin B1 gene duplication or deletion upstream the gene but the mechanisms of how the overexpression of a nuclear structural protein leads to such specific symptom as demyelination are still unclear. Considering the pivotal role that glial cells as astrocytes and oligodendrocytes and Leukemia Inhibitory Factor (LIF) have in the myelination process, this work was intended to analyse the morpho-functional aspects of different cell populations, which are engineered cellular models overexpressing Lamin B1 and primary cells deriving from ADLD patients. The results have, to date, highlighted that the astrocytes may be pivotal in the development of the disease. Analysing the cellular ultrastructure, astrocytes overexpressing Lamin B1 show several nuclear alterations similar to the ones observed in cells deriving from ADLD patients, which, on the contrary are not present in oligodendrocytes overexpressing Lamin B1. In addiction astrocytes overexpressing Lamin B1 are not capable to produce LIF and besides the receptor (LIF-R) is downregulated, it is downregulated as well as in oligodendrocytes overexpressing Lamin B1. In both engineered models, the confirmation that this signalling pathway is altered in the cell overexpressing Lamin B1, is given to us by analysing the signalling transduction pathways downstream LIF/LIF-R. In fact, both PI3K/AKT and JAK/STAT3 axes are downregulated but surprisingly with exogenous LIF administration is

possible recovered the phenotype. In particular, the toxic effect induced by Lamin B1 accumulation results in the ability of oligodendrocytes, being less affected, to completely recover the phenotype, which instead is only partial for astrocytes. Therefore, this leads us to hypothesize that astrocytes, being severely affected by Lamin B1 accumulation, lose their role of support for the oligodendrocytes in the myelination process. Finally, inflammation and ROS production was also been found in ADLD patients' cells as alleged in literature in relation to the Lamin B1 accumulation and advancement of age. These new discoveries both as regards cellular, morphological and functional alterations, and as regards the inflammatory process and oxidative stress could pay the way for new avenues of investigation in the ADLD disease.

Key words: Lamin B1, ADLD, astrocytes, LIF, cellular signalling

Abbreviations:

- ADLD Autosomal Dominant Leukodystrophy
- CNS Central Nervous System
- Erk Extracellular signal-regulated kinase
- GFP Green fluorescent protein
- GS3K Glycogen synthase kinase 3
- JAK Janus kinase
- IF Immunofluorescence
- LIF Leukemia Inhibitory Factor
- LIF-R LIF-Receptor
- LMNB1 Lamin B1
- MAPK Mitogen-activated protein kinase
- PNS Peripheral Nervous System
- PI3K Phosphatidylinositol-3 phosphate kinase
- STAT3 Signal transducer and activator of transcription protein 3
- TEM transmission electron microscopy

Introduction

1. Hereditary leukodystrophies and Autosomal Dominant Leukodystrophy

1.1. Hereditary leukodystrophies

Hereditary leukodystrophies are a heterogeneous group of rare and often progressive disorders, presenting with a wide range of symptoms and complications. The pathological bases that unite them are alterations of the glial cells or myelin sheaths leading to neuronal degeneration affecting the white matter or myelin tracts. Therefore, these diseases can occur with different degrees of demyelination at the level of the Central Nervous System (CNS) or Peripheral Nervous System (PNS) or both [1]. Myelin sheaths, characteristic elements of vertebrates, promote the propagation of electrical impulses along the axon of myelin fibres in the nervous system. This production is determined by specific cells, such as oligodendrocytes, for what concern the CNS, or Schwann cells in the PNS. In the CNS, oligodendrocytes are the largest producers of myelin through wrapping of their plasma membranes around axons or nerve fibres in a spiral manner. In this way oligodendrocytes ensure a rapid conduction of impulses in the nervous system as well as providing metabolic support to neurons [2]; just as astrocytes, which are equally important both in maintaining homeostasis of the CNS and as a supporter of the myelination process [3].

Numerous molecular mechanisms regulating the specification, differentiation and myelination of these cells of the nervous system have been identified, demonstrating that

possible failures in the regulation of these molecular processes may result in myelin malformation or degeneration resulting in several human diseases as the hereditary leukodystrophies or multiple sclerosis [4].

The most common example of hereditary leukodystrophy is the X-linked adrenoleukodystrophy (X-ALD, OMIM#300100) a genetic disorder that occurs primarily in males. It is caused by mutations in *ABCD1* gene, encoding for the adrenoleukodystrophy protein (ALDP) [5]. Since this protein is used for the transport of long chain fatty acids inside peroxisomes for their degradation, as a result of the mutation, a lipid accumulation occurs in all body tissues [6]. The resulting pathological phenotype may include an asymptomatic state, adrenergic insufficiency, cerebral demyelination in presence of inflammation and a progressive state of spastic paraparesis [7]. The prevalence of X-ALD is 1 in 20,000 to 50,000 individuals worldwide occurring with a similar frequency in all populations.

Another important example of hereditary leukodystrophy is the Krabbe's disease (OMIM#245200) that is due to a mutation in the GALC gene, which encodes for the lysosomal enzyme galactosilceramidase [7]. The genetic mutation leads to a decrease of the enzyme functionality and a white matter alteration both at the CNS and PNS level, resulting in spastic events, delay in development, and irritability. In the United States, Krabbe disease affects about 1 in 100,000 people and individuals with late-onset Krabbe disease may survive many years after the onset of the disease.

Finally, to mention another less common leukodystrophy, it must be remembered the Pelizaeus-Merzbacher Disease (PMD, OMIM#312080) another inherited condition that primarily affects males as in the case of the X-ALD. The prevalence of this disease is estimated to be 1 in 200,000 to 500,000 males in the United States. Genetically it exhibits mutation of the gene coding for proteolipid protein that is the major component of myelin

sheaths. At cellular level, oligodendrocytes, astrocytes, microglia and neurons are affected by several mechanisms [8]; the cellular alterations may determine, with different processes, initial nystagmus, hypotonia, cognitive problems, progressive ataxia and spasticity [7].

The Autosomal Dominant Leukodystrophy (ADLD, OMIM#169500) belongs to the leukodystrophies group and it will be illustrated in the next chapters, focusing on its characterizing clinical and genetic features.

1.2 ADLD: Nomenclature and Epidemiology

Autosomal Dominant Leukodystrophy is a rare, fatal and late onset slowly progressive demyelinating disorder, which affects the white matter of the central nervous system.

It was originally known as "autosomal dominant leukodystrophy mimicking chronic progressive multiple sclerosis" and "adult-onset leukodystrophy simulating chronic progressive multiple sclerosis" [9] [10] . The most known names to date are “Adult-onset autosomal dominant Leukodystrophy” or more commonly “Autosomal Dominant Leukodystrophy” abbreviated as ADLD.

The disease presents in the fourth to fifth decades of adulthood without any gender differences. Penetrance is not known yet but is assumed to be 100%; also, the prevalence is unknown. Published cases include 24 different families with more than 70 affected individuals and with different origins:

- Irish-American[11]
- Italian[12] [13]
- Japanese[1]
- Swedish[14]
- French-Canadian[15]
- Israeli[16]
- German[17]
- Serbian [18]

1.3 ADLD: the genetic basis

ADLD is an inherited disease. The first linkage studies was conduct by Coffeen at all. in 2000 by discovering that the abnormal gene causing the ADLD disease is localized into chromosome 5q31 [19]. Later, Padiath at al., by analysing the same kindred used by Coffeen and another Irish American kindred, were able to identify that this region presents an extra copy (duplication) [1], tandemly oriented in a head to-tail manner, of the *LAMIN B1* gene (*LMNB1*) on 5q23.2 chromosome [1]. Further studies, carried out on 20 ADLD total families, have shown that a duplication of 72 kb of *LMNB1* is sufficient to define the pathological phenotype [20]. The *LMNB1* gene encodes for the nuclear laminar protein called Lamin B1 [1]. In ADLD patients, a duplication of *LMNB1* is associated with an increase of Lamin B1 protein levels, confirmed by several analysis of RNA and protein expression conduced in post mortem patient's brain tissue. This would be the genetic classification to identify an ADLD patient except that Brussino et al. in 2009 described a new family with a genetic defect in 5q23 chromosome without copy number mutations [13]. Independently to that, when Lamin B1 mRNA expression levels were analysed, the expression were significantly increased in ADLD patients compared to controls, leading to the conclusion that a cis-acting regulatory mutation may have led to the increased mRNA levels [21]. As a result from the etiological point of view, it can be said that ADLD is caused by chromosomal rearrangements that regardless of whether it is duplication of the *LMNB1* gene (5q23.2) or deletion upstream of the gene, it causes an increase in the expression level of Lamin B1, which is responsible for the ADLD disease phenotype [22] (*Figure 1*).

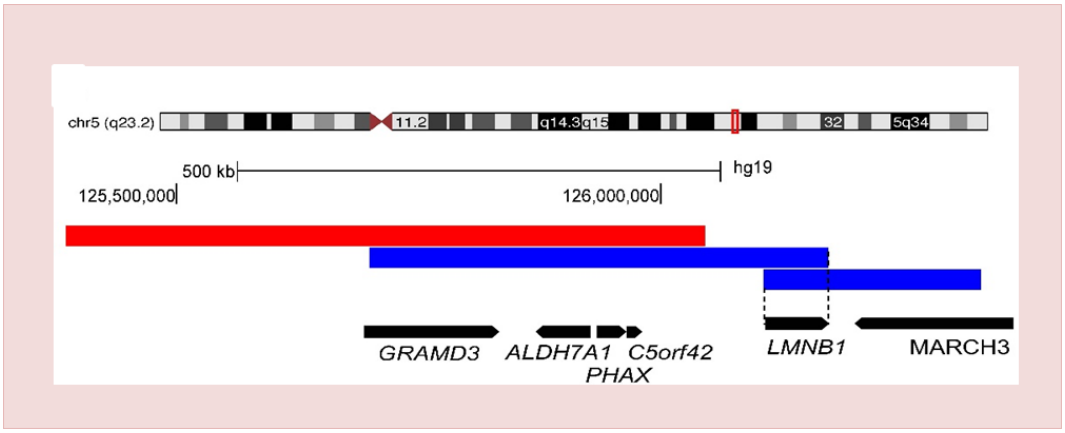

Figure 1 *Genomic region on chromosome 5q23.2 containing the LMNB1 gene. The blue bar are representative for the genomic duplications in two different ADLD patients showing the centromeric and telomeric junctions near to the LMNB1 gene, the minimal critical region required for ADLD disease (dashed line). The red bar indicates the deletion upstream the LMNB1 gene and in black the location of genes having genomic rearrangements and the direction of transcription.*

1.4 ADLD: clinical signs

ADLD was described for the first time in 1984 by Eldridge et al. in a large Irish American family [9]. Affected members showed progressive and fatal neurological disorders at the expense of the white matter in the CNS, without any involvement of neurons, such as Purkinje cells [9].

Subsequently similar phenotypes, deriving from different ethnicities, has been found in a Japanese [23], Italian [12], French[24] and Swedish family [14].

Before reaching the genetic cause, the characteristics that united these groups were generally due to the phenotypic observation attributable to autonomic dysfunction from bladder or bowel to orthostatic hypotension, temperature dysregulation, and anhidrosis [11]

[21]. The primary autonomic symptoms are followed by cerebellar dysfunction (ataxia, dysmetria, nystagmus, tremor) and pyramidal defects (spasms and weakening of the limbs)[4],as well as, in some cases, cognitive, auditory and visual defects were also encountered [10 22].

For a long time, before the use of Magnetic Resonance Imaging (MRI) or computerised axial tomography, ADLD patients were diagnosed as having chronic progressive multiple sclerosis (MS) [11]. The use of MRI was the first method which allowed the experts to distinguish ADLD patients from MS patients [25], and currently MRI is still one of the first analysis technique used for the identification of this rare disease. In ADLD patients compared with MS presents, MRI imaging shows widespread and symmetrical degeneration of white matter in the CNS. This deterioration starts from the motor cortex to the medulla oblongata and leads to the following involvement of the upper and middle cerebellar peduncles [13 19 26]. Histopathologically, white matter abnormalities in superiomedial portions of the frontal and parietal lobes have been described, also some involvement of the corpus callosum, cerebellar peduncles and the hemispheres, underlining an important vacuolar demyelination processes at the light microscopy observation [19 27 22] .

Besides this, the ADLD can be distinguished from MS through the study of family history, which suggests an autosomal dominant inheritance mechanism [9]. Indeed, unlike ADLD (highly penetrating, autosomal dominant and adult onset disease), the most hereditary leukodystrophies present as autosomal recessive or recessive pathologies related to the X chromosome and the age of onset is typically childhood as for adrenoleukodystrophy, Krabbe's disease and PMD [1]. In addition, other distinctive symptoms that allow to distinguish ADLD from MS are:

- the initial autonomic dysfunction, element never found in MS patients;

- the extensive and symmetric demyelination, which in MS is asymmetrical;
- the absence of an immune response directed against the myelin protein with consequent inflammation;
- neuropathology does not present phenomena of astrogliosis and there is the maintenance of oligodendroglia, although in the presence of subtotal demyelination [19] *(Figure 2).*

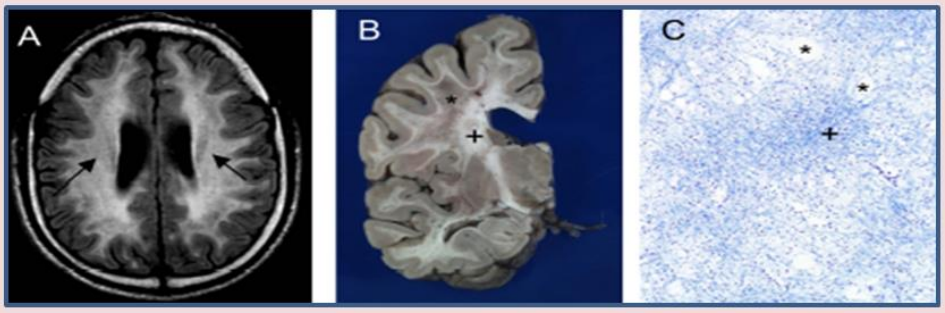

Figure 2. *(A) Magnetic resonance imagining (MRI) of ADLD patient brain showing intensities symmetrical white matter extending from the motor cortex to the medulla oblongata and the involvement of the upper and middle cerebellar peduncles, marked by arrows, indicating myelin defect. (B) ADLD patient brain showing irregular areas of myelin loss marked by asterisk (*) respect areas of normal myelin marked by plus sign (+). (C) ADLD brain section analysed using a myelin stain showing areas of vacuolar demyelination marked by asterisks (⁎) compared to normal myelin staining indicates with plus sign (+).*

2. Lamin B1 alterations

The nuclear lamina is a protein three-dimensional structure of fibrous meshwork of intermediate filaments (IFs) that underlie the inner nuclear membrane [28]. In mammalian cells it is composed by four major types of different lamins:

- The A-type lamins, including pre- lamin A, lamin A and C which are alternate splice forms of the same gene *LMNA*, on 1q21 chromosome [29] [30].
- The B-type lamins, comprising lamin B1 and B2, coded by separate *LMNB1* and *LMNB2* genes, on 5q23 and 19q13 chromosomes [31].

Based on their structural characteristics and their amino acid sequence, lamins are classified as intermediate filaments of type V. Like other IFs they are fibrous proteins that join together forming filaments presenting central α-helical rod domains and a variable head and tail domains. Initially two α-helices wrap around each other in parallel to form a lamin-lamin dimer, the basic filament building block, then these dimers are associated with many others both in head-tail direction and laterally to generate the final structure [32]. (*Figure 3*)

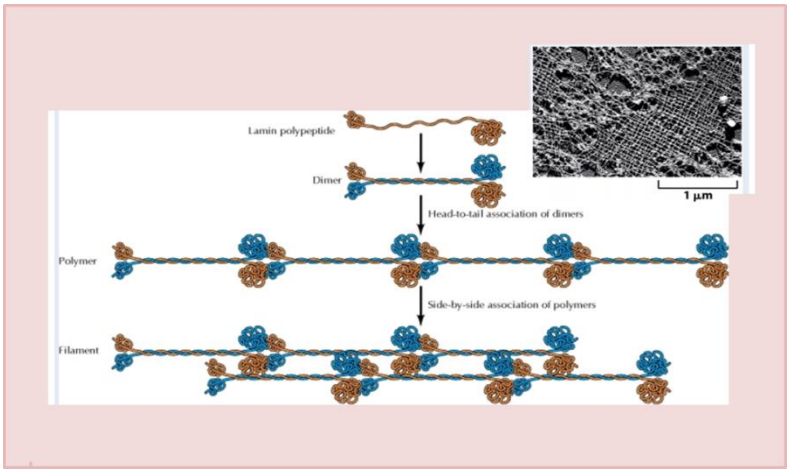

Figure 3. This image is composed by an image detected by transmission electron micrograph showing the nuclear lamina meshwork of nuclear envelope spread from Xenopus oocytes. Scale bar = 1 µm. Copyright Nature Publishing group; and by schematic representation of a nuclear lamin assembling where two lamin polypeptides create the nuclear lamin dimer through the ability to form two-stranded -helical coiled coils, wrapped around each other, then the nuclear lamin dimers associating in a head-to-tail manner form polymers and finally the formation of Filaments.

Originally, it was believed that nuclear lamina was a passive structural component of the cell, able to provide only integrity to the nucleus. Later, several studies have demonstrated that nuclear lamina plays multiple and dynamic functional roles in numerous cellular process [33] [34], giving structural support to the nucleus and playing dynamic roles in the regulation of chromatin, during the transcription, DNA replication and regulating epigenetic phenomena[35].

Mutations in genes encoding for nuclear lamina have been described in a large number of diseases, most of which are associated with lamin A/C alteration and called “laminopathies”.

ADLD is the first disease, linked to Lamin B1 mutations, that leads to an enrichment of the role played by nuclear lamina and its involvement in nervous system disorders. Although Lamin B1 is present in different cell types, its activity is most important during neural

development and for brain functions in adulthood [4]. Consequently, modifications that alter its expression are attributable to adverse effects for cell survival as described below. An important function of Lamin B1 is the regulation of gene expression through the association with specific transcription factors such as sterol response element binding protein 1 (SREBP1) or the octamer transcription factor (Oct-1) [36]. The latter, in particular, is an important factor for the regulation of genes involved in response to oxidative stress and co-localizes with Lamin B1. In mouse model, it was demonstrated that Lamin B1 deficiency leads to a dysregulation of Oct-1-dependent genes causing an increase of reactive oxygen species (ROS) [36], which are very toxic for the cell, and that cause a harmful and irreversible effect on it. In equal measure also, an overexpression of Lamin B1 leads to several consequences. Several studies on human (HEK 293) and murine (Ng2a) cell lines, have shown that, Lamin B1 overexpression through the increase of the protein level, leads to an increase in the nuclear rigidity and this is also found in the nuclei of epithelial fibroblasts of ADLD patients [37].

As well as nuclear structural changes [38], Lamin B1 accumulation in relation to several stress conditions was also linked with senescence [39], as observed in Ataxia telangiectasia (A-T) cells, an autosomal-recessive genetic disorder. The oxidative stress, causing Lamin B1 overexpression, leads to an alterations of the nuclear shape, and considering the failure to reduce the reactive oxygen species, the cell goes towards an early senescence [39].

Although Lamin B1 accumulation has been linked to both nuclear structural changes and senescence, its role is still controversial, challenging and tissue- specific [40–43]. In ADLD disease, despite the genetic causes, the molecular aspects of this pathology are not clear yet and the disruption of the myelin seems to be the most significant aspects of the disease.

3. Molecular and cellular mechanisms implicated in the myelination process

The mechanisms regulating myelination are still unclear. Myelin is formed by the extension of oligodendrocytes cell membranes, which wrap around the axons of neurons in a spiral manner. It is composed for the 70–80% by lipid and 20–30% by protein. The most abundant proteins are myelin basic protein (MBP) and proteolipid protein (PLP1) which together constitute 80–90% of total myelin protein. The remaining part is composed by myelin-associated glycoprotein (MAG) and myelin oligodendrocyte glycoprotein (MOG) [44] [45].

Myelination process begins during late stages of fetal development and continues into early adult life [46]. In the CNS of vertebrates, until recently, the saltatory nerve conduction was considered the only purpose of myelin [47], on the contrary, currently, it is know that myelin is implicated in several cellular function, by providing metabolic support to neurons [48], regulating ion and water homeostasis, and adapting to activity-dependent neuronal signals [49].

Oligodendrocyte cells, are certainly the primary cells responsible for myelinating axons [50], but signals deriving from astrocytes and neurons are also essential to promote myelin formation and its maintenance during the life [51].

Astrocytes, in particular, play an important role supporting myelination [3] through the secretion of several factors. Among these soluble factors there are: platelet-derived growth factor (PDGF), basic fibroblast growth factor (FGF2), insulin-like growth factor 1 (IGF-1),

ciliary neurotrophic factor (CNTF), metalloproteinase-1(TIMP-1), and endothelin-1 (ET-1) and Leukemia Inhibitory Factor like protein (LIF) [49].

Leukemia Inhibitory Factor (LIF), compared to these molecules studied in the CNS, arouses particular interest for what concern the myelination process and, therefore, it is classified as a pro-myelinating factor [46]. LIF is a multi-functional cytokine belonging to the interleukin 6 (IL-6) superfamily. Its name derived from the discovery of this factor able to induce the differentiation of murine M1 myeloid leukaemia and macrophage maturation to suppress leukaemia proliferation [52]. It can regulate several biological processes, through both autocrine and paracrine signalling, including differentiation of leukaemia cell, neuronal development, inflammatory response, stem cell self-renewal and cancer progression [53]. It is extensively studied in neuronal development, because of its influence on neuronal survival and differentiation in the peripheral nervous system, its involvement in the induction of the switch of neurotransmitter expression in sympathetic neurons and because of its ability to induce sensory neurons in response to trauma but especially for the stimulation of the glial development [54] .

LIF binds to its specific receptors with high affinity, the heterodimeric glycoprotein 130 (gp130)/LIF receptor (LIFR) complex. This specific binding leads to the activation of 3 main signal transduction pathways: the Janus kinase/signal transducer and activator of transcription protein 3 (JAK/STAT3), phosphatidylinositol-3 phosphate kinase (PI3K/Akt) and mitogen-activated protein kinase MAPK/ERK1/2 pathways [55]. The activation of these 3 pathways promote cell growth , proliferation and survival but in particular, this signal pathways promote the survival and differentiation of oligodendrocytes delivering the myelination process [3] .

4. LIF signal transduction pathways: JAK/STAT, PI3K/Akt and MAPK/ERK signalling.

Upon LIF binding to its specific receptor gp130/LIFR, three main signalling pathways can be subsequently activated: JAK/STAT, PI3K/Akt and MAPK/ERK signalling (*Figure 4*). The activation by phosphorylation of each signalling pathway is different for each cell types, but they are essential to promote actions in which LIF exerts its effect, such as: change of gene expression, cell survival and an anti-apoptotic effect [56]. Several studies conducted on embryonic stem cell, have demonstrated that JAK/STAT signalling controls genes that regulate self-renewal, PI3K/Akt signalling controls genes implicated in cell pro-survival and MAPK/ERK signalling controls genes involved in proliferation and self-renewal [57]. For what concern the regulation of neuronal signalling, one of the most important roles played by LIF through these signalling pathways is the development and maturation of glial cells and neurons, indeed it can:

- promote the maturation of astrocytes from astrocytic progenitor cells;
- facilitate the development of mature oligodendrocytes from OPCs;
- rescue grey and white matter from damage preventing neuronal and oligodendrocyte loss;
- promote neuroprotection after focal cortical injury upregulating antioxidant enzymes in oligodendrocytes and neurons;

Even if the molecular mechanisms are not clear yet, several studies have demonstrated that if the gp130 receptor is genetically removed from astrocytes, astrocyte cannot survive and large areas of demyelination begin to form inducing additionally a pro inflammatory T cell response [58]. In addiction during CNS injury, infection and inflammation, it was demonstrated that astrocytes operate in neuro-regeneration and re-myelination, increasing the expression of LIF and preventing oligodendrocytes apoptosis [59].

This event, poorly studied yet, underlying the important cross-talk between astrocytes and oligodendrocytes, not only in healthy conditions but also in disease, and, considering that they are the primary cells involved in the myelination process, additional studies need to be conducted.

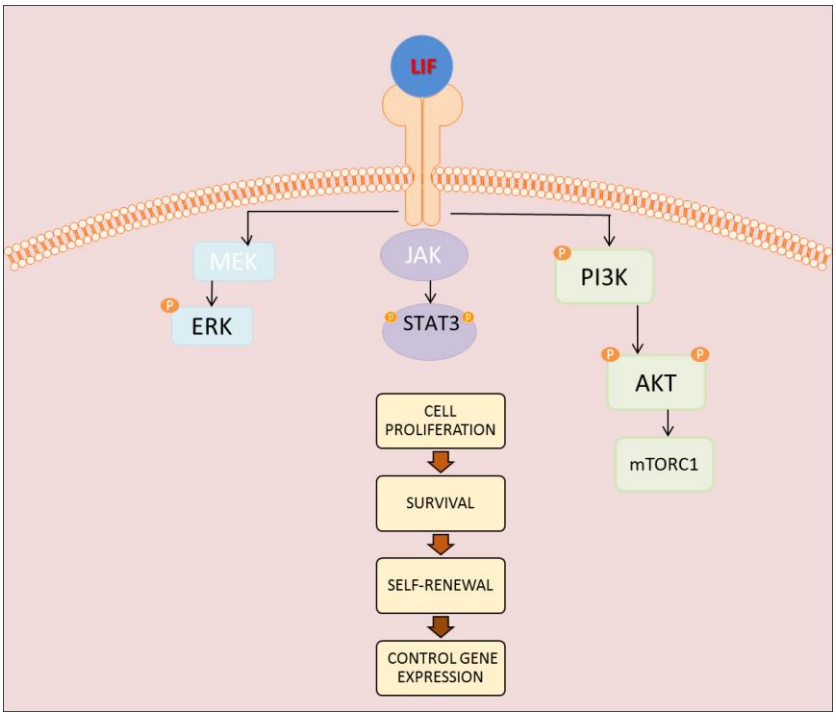

Figure 4. *LIF signal transduction pathways. Representative image when LIF binds its receptor LIF-R and subsequent activation of 3 essential axes: PI3K/AKT, JAK/STAT3 and MAPK/ERK1/2 which are implicated in cell proliferation, survival, self-renewal and control of gene expression.*

5. ADLD: where are we now

Considering that demyelination is the primary condition in ADLD, astrocytes and oligodendrocytes are the obvious candidate targets to investigate the molecular mechanism at the base of the disease, also knowing the interdependence that these cells have in the myelination process.

Histopathologically, the first analysis of ADLD patient brains, showed that oligodendrocytes and neurons did not possess any alternations in morphology and in cell number compared with astrocytes, that showed an abnormal beading and shortening of their processes [19]. In other studies, instead, it was observed that the overexpression of Lamin B1 in oligodendrocytes, leads to a premature arrest of oligodendrocytes differentiation with a reduction of MBP and PLP1 protein; on the contrary no alterations were observed in astrocytes after the overexpression of Lamin B1 [60]. Even murine models have not been able to clear up this dilemma. Indeed, the most recent model created with the Lamin B1 overexpression at oligodendrocytes level, was capable of recapitulating the age-dependent motor signs, but not the early autonomic cardiovascular dysfunction, primary sign of ADLD [61]. Transgenic mouse models overexpressing *LMNB1* in oligodendrocytes were created by other two groups [62] [63]. The group of Heng et al. have suggested that demyelination could be due to a lower transcript levels of myelin genes [63]. However no changes in myelin gene transcripts were found by the group of Rolyan et al., who nevertheless identified alterations in the lipid composition [62]. To support these data, Yattah et al. were able to identify *Lss* gene encoding for lanosterol synthase, a key enzyme in cholesterol synthesis, whose expression was inversely related to Lamin B1 levels and which is critical for the lipid metabolism [64]. As

latest data, it has been proposed in 2019 by E. Giorgio e al. the use of ASP-siRNA (allele-specific silencing by RNA interference) as a therapeutic strategy to target the non-duplicated allele of the LMNB1 gene with the aim to reduce the high protein expression level close to wild-type levels [65]. The use of interfering RNA treatment has abrogated the ADLD-specific phenotypes in fibroblasts and in two cellular models: neurons reprogrammed from patients' fibroblasts and murine oligodendrocytes overexpressing human *LMNB1*. However, it was not possible to reproduce the same experiment in a mouse model, because the two mouse models currently available (Lmnb1BAC and PLP-LMNB1Tg) are not suitable for this experiment [63 66].

This evidence suggests that is difficult both to create an *in vivo* model and to pinpoint the really cell type which suffer for the increased Lamin B1 expression, for these reasons further studies are required. Therefore considering the pivotal and complicated role that Lamin B1 exerts in nuclear structure maintenance [67] , and considering the cellular processes and the important role that astrocytes, oligodendrocytes and LIF have in the myelination of CNS [4], the understanding of new possible signalling pathways related to the ADLD pathology need to be deepened.

Aim of the work

It is still a great challenge understanding how the overexpression of a nuclear structural protein determines such a specific symptom as demyelination. To date, the data reported in the literature are not sufficient to explain the molecular mechanisms that lead to ADLD disease therefore the understanding of new cellular and molecular mechanisms is mandatory in order to develop a specific therapeutical approach.

For this reason, my PhD project aimed to validate a cellular model able to overexpress Lamin B1 and to study its effect primarily for what concerns cellular signalling and morphological alterations. In particular, we focused on:

- Creating two ADLD experimental models by overexpressing Lamin B1 in the oligodendrocytic cell line MO3.13 and in the astrocytic cell line U87-MG, both cell types typically involved in myelination processes.
- Identifying a possible molecular target implicated in the myelination process.
- Analysing alterations in signal transduction pathways.
- Characterising fibroblasts derived from ADLD patients and healthy donors.

Materials and Methods

Cell Culture

The following cell lines were used:

- **U87-MG** Human glioblastoma astrocytes (HTB-14 ATCC, Old Town Manassas, Virginia, US), cultured in EMEM (Corning, New York, US) with 10% FBS and 1% Penicillin/Streptomycin (Sigma-Aldrich, Missouri, US).
- **MO3.13** Human Oligodendrocytic cell line (Cedarlane Laboratories, Burlington, Canada), cultured in DMEM (Corning, New York, US) supplemented with 10% FBS and 1% Penicillin/Streptomycin, without sodium pyruvate.
- **HEK 293Ta** (Genecopoeia Inc, US) Lentiviral Packaging cell line derived from human embryonic kidney, were cultured in DMEM (Corning, New York, US) with 10% FBS and 1% Penicillin/Streptomycin, however, 5% FBS was used during transfection.
- **Primary human dermal fibroblasts** isolated from skin biopsies of six ADLD patients carrying *LMNB1* gene duplication and six healthy donors, obtained from the IRCCS Istituto delle Scienze Neurologiche di Bologna, UOC NeuroMet, Italy. Human primary fibroblasts were grown in DMEM supplemented with 10% FBS and 1% Penicillin/Streptomycin.

  This study was approved by the AUSL Bologna Ethical Committee and informed consents were obtained from all participants.

All cells were maintained in a humidified incubator at 37 °C with 5% CO2.

Lentiviral transduction

In order to produce lentiviruses to overexpress both LMNB1 and green fluorescent protein (GFP) for our disease model, as well as, lentiviruses coding only for GFP as control, EX-I3724-Lv201 vector coding for Homo Sapiens LMNB1 and EX-NEG-Lv201 vector for empty control (Genecopoeia Inc, US) were used.

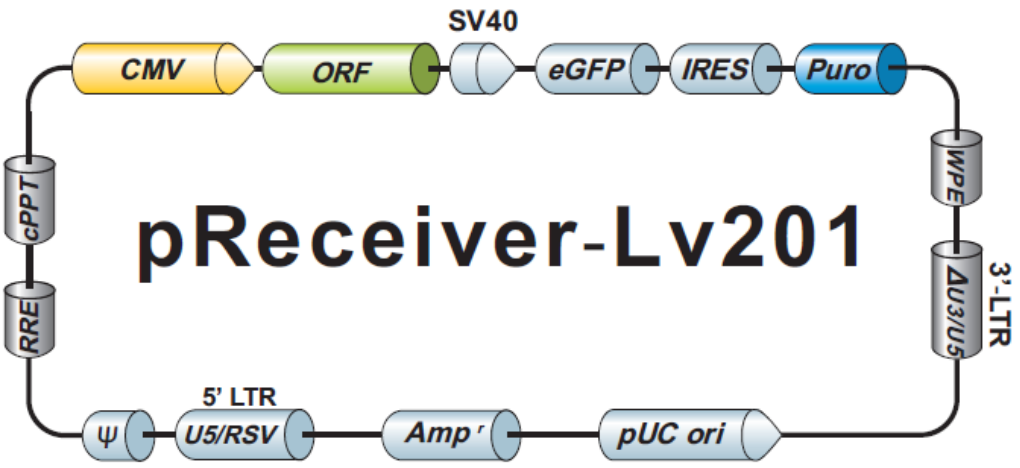

Figure 1. Vector used to overexpress Lamin B1

According to manufacturer's protocol, the Lenti-Pac HIV expression packaging kit (Genecopoeia Inc., US) was used to transfect HEK293Ta packaging cells. The transfection mix was composed by adding to OptiMEM®: 1 μg of target vector DNA, 0.57 μg of Gag-pol vector, 0.28 μg VSV-G vector, 6μl of PEI (*protonation of polyethylenimine*) to have a total

DNA:PEI ratio of 1:3. 24 hours and 48 hours after incubation, the supernatants containing the virus were collected respectively and used for the transduction of U87-MG, MO3.13 and fibroblasts cell lines or alternatively stored at -80°C.

48 hours after transduction, U87-MG, MO3.13 and fibroblasts were selected for 48 hours in growth media supplemented with 2 μg/ml of puromycin (Sigma-Aldrich, Missouri, US) for U87-MG cells, 1 μg/ml of puromycin for MO3.13 cells and 1,5 μg/ml of puromycin for fibroblasts.

LIF administration

In order to test the ability of LIF to rescue the normal phenotype following Lamin B1 overexpression, U87-MG and MO3.13 cells were treated with 80 ng/ml of Recombinant Human Leukemia Inhibitory Factor, LIF (Thermo Fisher Scientific) 48 hours post transduction for 48 hours (96 total hours) [68].

RNA extraction, Reverse Transcription and Real-time PCR

The extraction of total RNA from samples was made by using RNeasy Mini Kit (Qiagen, Hilden, Germany) and the Nanodrop spectrophotometer was used to quantify extracted RNA. 1μg of total RNA was reverse transcribed into cDNA using the iScript gDNA Clear cDNA Synthesis Kit (Bio-Rad, Hercules, California, US), following the manufacturer's protocol.

mRNA expression levels were evaluated using a TaqMan probe-based real-time PCR system (Thermo Fisher Scientific, Waltham, Massachusetts, US). Real-time PCR was performed using 100 ng of cDNA per well, with the ABI PRISM 7300 real-time PCR machine (Applied Biosystems, Life Technologies, Carlsbad, California, US) and GAPDH was used as housekeeping gene. Data are presented as fold changes relative to expression levels of control samples in accordance with the $2^{-\Delta\Delta CT}$ formula. Validated gene probes used are as follows: LMNB1 Hs.PT.58.40133522, LIF Hs.PT.58.27705899, LIF-R Hs.PT.58.2980475, GAPDH Hs.PT.39a.22214836 (IDT, Coralville, Iowa, US).

Protein Extraction and Western Blot

Cells were lysed with T-PER (Thermo Fisher Scientific®) lysis buffer supplemented with Halt protease and phosphatase inhibitor cocktails (Thermo Fisher Scientific, Waltham, Massachusetts, US). Lysed cells were sonicated in 1 cycle of 15 seconds duration and at a power of 40-50% and finally were quantified with the Bradford Protein Assay (Bio-Rad, Hercules, California, US). 40 µg of total proteins were separated on Bolt 4-12% polyacrylamide-0.1% commercial SDS gels (Thermo Fisher Scientific, Waltham, Massachusetts, US) and transferred onto nitrocellulose membrane. Membranes were washed with PBS-0.1% Tween-20 (PBST) and non-specific binding sites were blocked with blocking buffer (5% w/v non-fat dry milk in PBST) for 1 hour at room temperature and incubated with primary antibodies overnight at 4°C. On the basis of manufacturer's protocols, the antibodies used were diluted 1:1000 in either bovine serum albumin (BSA) or milk, washed again with PBST and lastly incubated with peroxidase conjugated secondary

antibodies (Thermo Fisher Scientific, Waltham, Massachusetts, US) diluted in PBST for 1 hour at room temperature. ECL enhanced chemiluminescence reagents (Thermo Fisher Scientific, Waltham, Massachusetts, US) were used for the bands detection and the images were captured with the ChemiDoc-It®2Imager digital system (UVP, Upland, California US).

Immunocytochemistry

Cells were fixed in ice-cold 100% methanol (Sigma-Aldrich, Missouri, US) for 15 minutes at -20°C. After blocking in 1% bovine serum albumin (BSA) for 1hour at room temperature, cells were incubated with primary antibody overnight at 4 °C following the manufacturer's instructions. Lastly, cells were incubated in the dark at room temperature for 1 hour with corresponding secondary antibodies, Anti-Mouse IgG F(ab')2 Fragment antibody conjugated to Alexa Fluor 488 (Cell Signaling Technology, Leiden, The Netherlands) or Anti-Rabbit IgG F(ab')2 fragment-Cy3 antibody (Sigma-Aldrich). Lastly, nuclei were stained with ProLong Gold Antifade reagent with DAPI (Invitrogen, Thermo Fisher Scientific). Slides were then examined under a Zeiss Axio-Imager Z1 fluorescent microscope (Carl Zeiss International, Germany). At least five different fields were analysed at 20X magnification.

Antibodies

Antibodies used in western blotting and immunofluorescence analysis

Lamin B1	(10H34L18) Invitrogen, Thermo Fisher Scientific
LIF	(PA5-21122) Invitrogen, Thermo Fisher Scientific
PI3K p110α	(CST 4249) Cell Signaling Technology (Danvers, MA, US)
PI3K p110γ	(CST 5405) Cell Signaling Technology (Danvers, MA, US)
phospho - Akt	(CST 9271) Cell Signaling Technology (Danvers, MA, US)
Raptor	(CST 2280) Cell Signaling Technology (Danvers, MA, US)
phospho - Stat3	(CST 9134) Cell Signaling Technology (Danvers, MA, US)
PKCα	(PA517551) Invitrogen, Thermo Fisher Scientific
phospho - GSK3α/β	(CST 8566) Cell Signaling Technology (Danvers, MA, US)
phospho – p44/42 MAPK	(CST 4695) Cell Signaling Technology (Danvers, MA, US)
phospho - Stat4	(71-7900) Invitrogen, Thermo Fisher Scientific
phospho - NFkB	(CST 3033) Cell Signaling Technology (Danvers, MA, US)
β-Tubulin	(T7816) Sigma-Aldrich

Enzyme-Linked Solid Phase Immunosorbent (ELISA) Assay

The concentration of human LIF in growth medium of cultured cells was detected using the Human LIF ELISA Kit assay (Invitrogen, Thermo Fisher Scientific).48 hours after transduction, cells were puromycin-selected for other 48 hours and 2.5 x 10^5 cells were seeded per well in a 12-well plate. The next day, supernatants were collected and centrifuged for 10 minutes

at 6,000 x g. Following the manufacturer's instructions, a dilution 1:2 was performed for each supernatant before assaying in triplicate wells. For each sample (wild type, empty vector and *LMNB1* overexpressing cells), three supernatants obtained from three separate experiments were assayed. To read absorbance at 450nm (primary wavelength) and at 620nm (reference wavelength) it was used Glomax Discover (Promega, Madison, Wisconsin, US). Analysed data are presented as Mean ± Standard Deviation.

Transmission Electron Microscopy (TEM) analysis

U87-MG, MO3.13 cells and primary healthy donors and ADLD patients fibroblasts were fixed with 2.5% glutaraldehyde in 0.1M cacodylate buffer, for 2 h at 4°C and then, post fixed in 1% O_sO_4 in 0.1 M cacodylate buffer, for 30 minutes at room temperature. After few washes in 0.15 M cacodylate buffer, samples were dehydrated through graded acetone solutions and embedded in Epoxy resin (Sigma Aldrich, St. Louis, Missouri, US). Sections of 100 nm each were collected in nickel grids, counterstained with 3% uranyl acetate and 1% lead citrate and observed by Philips CM10 TEM (FEI Company, Eindhoven, The Netherlands), at an accelerating voltage of 80 kV. Images were recorded by Megaview III digital camera (FEI Company, Eindhoven, The Netherlands).

Quantitative analysis of misshaped nuclei

Primary fibroblasts grown on cover glasses and processed for immunofluorescence labelling were used for a quantitative analysis of misshaped nuclei compared to regular nuclei between healthy donors and ADLD patients. Quantitative analysis was performed on 100 nuclei of cultured fibroblasts from each patient, at 60X magnification. The number of misshaped nuclei was compared to regular nuclei and results were expressed as average value (± SD), in percentage, and they were graphically represented for ADLD patients and healthy donors.

ROS production assessment

Intracellular reactive oxygen (ROS) species production was tested in primary fibroblasts using the cell-permeant probe 2'-7'-dichlorofluorescein (H2DCFDA), a nonfluorescent reduced form of fluorescein, which becomes fluorescent upon cleavage by intracellular esterases and oxidation by ROS. The fluorescence was monitored with GloMax® Discover Microplate Reader Technology using 475 nm (blue) as excitation wavelength and 500-550 nm emission wavelength.

The probe was dissolved in DMSO to obtain a 5 mM solution, kept at -20°C and aliquoted in amber micro-tubes to protect it from light-induced oxidation, until the preparation of the fresh 5µM ready-to-use solution. 4.5 x 10^5 fibroblasts/sample were washed twice and resuspended in 450 µl of PBS. To assess autofluorescence, 150 µl of the sample were used and the remaining cells were incubated for 10 minutes at 37°C with 5µM H2DCFDA, in order

to load the fluorescent probe. After incubation, 150 µl of fibroblast suspension were left untreated to measure basal ROS production while 150 µl were treated with 300 µM H_2O_2 to evaluate the oxidative activity in response to a stimulus. 50 µl of fibroblasts suspension were seeded per well in a black 96-well plate. For each triplicate sample, the autofluorescence, basal ROS production, and ROS production following H2O2 treatment were analysed. Fluorescence was measured in a time course every 15 minutes for 7 hours, after brief shaking.

Statistical Analysis

Statistical analysis was carried out using GRAPH PAD PRISM 5.0 software (San Diego, CA, US) by applying the two-way ANOVA and Sidak post-test. The differences were considered significant with $p < 0.05$*, $p < 0.01$ ** and $p < 0.001$ ***.

Results

In vitro models

1. Astrocytic and oligodendrocytic cell lines

1.1. Evaluation of Lamin B1 overexpression and localization.

In order to study the effect of Lamin B1 overexpression, astrocytes U87-MG and oligodendrocytes MO3.13 cell lines were transiently transduced with lentiviral infection. After puromycin selection, cells were tested for Lamin B1 expression both at mRNA and protein levels and compared to wild type (WT) and cells transduced with an empty vector coding only for green fluorescent protein (GFP). In addition, Lamin B1 nuclear localization was evaluated by immunofluorescence (IF) **(Fig. 1).**

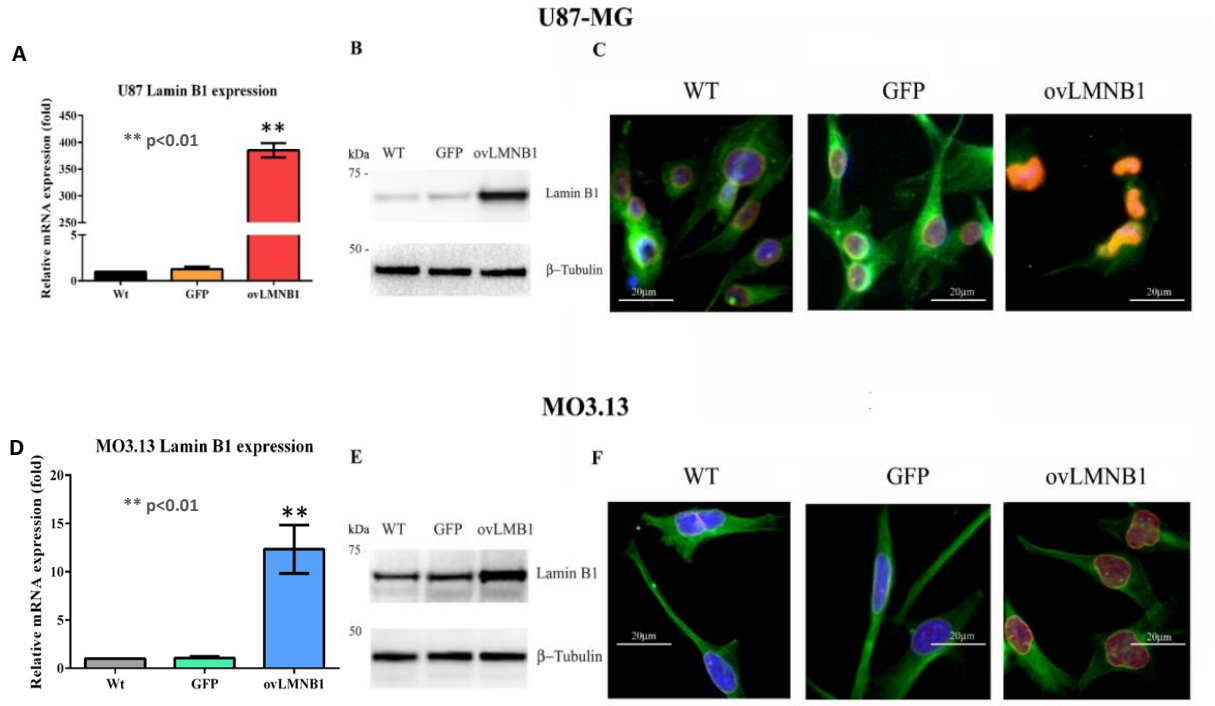

Figure 1 Evaluation of Lamin B1 overexpression in U87-MG and MO3.13 through qRT-PCR, Western blot analysis and immunofluorescence. Results are representative of 5 different experiments.

After 96-hour transduction, both overexpressed cell lines (ovLMNB1) show high levels of Lamin B1 mRNA and protein compared to WT and GFP (**Fig. 1A, 1B, 1D**, **and 1E**). The expression levels of Lamin B1 are greater in U87-MG (**1A-1B**) than in MO3.13 cells (**1D-1E**). Also the IF analysis (**1C-1F**) confirmed an increased immunoreactivity in transduced cells (ovLMNB1) compared to controls WT and GFP and this confirmed the different levels of overexpression reached in the two cell line models: U87-MG astrocytic cell line being the one showing higher levels of Lamin B1 overexpression. Additionally, IF images show that Lamin B1 is localized in the nucleus, particularly in the nuclear lamina and nucleoplasm, both in transduced U87-MG and in MO3.13 with evident alterations in the nuclear shape of U87-MG cells compared to MO3.13 following Lamin B1 accumulation. GAPDH and β-tubulin were used respectively as housekeeping gene and loading control. For the immunofluorescence, Lamin B1 is marked in red and β-tubulin in green. 20X magnification (bar:20μM).

1.2. Lamin B1 overexpression affects nuclear morphology in U87-MG cells

The nuclear morphology was evaluated by transmission electron microscopy (TEM) (**Fig. 2**) and nuclear shape was examined both in U87-MG and in MO3.13 cell lines.

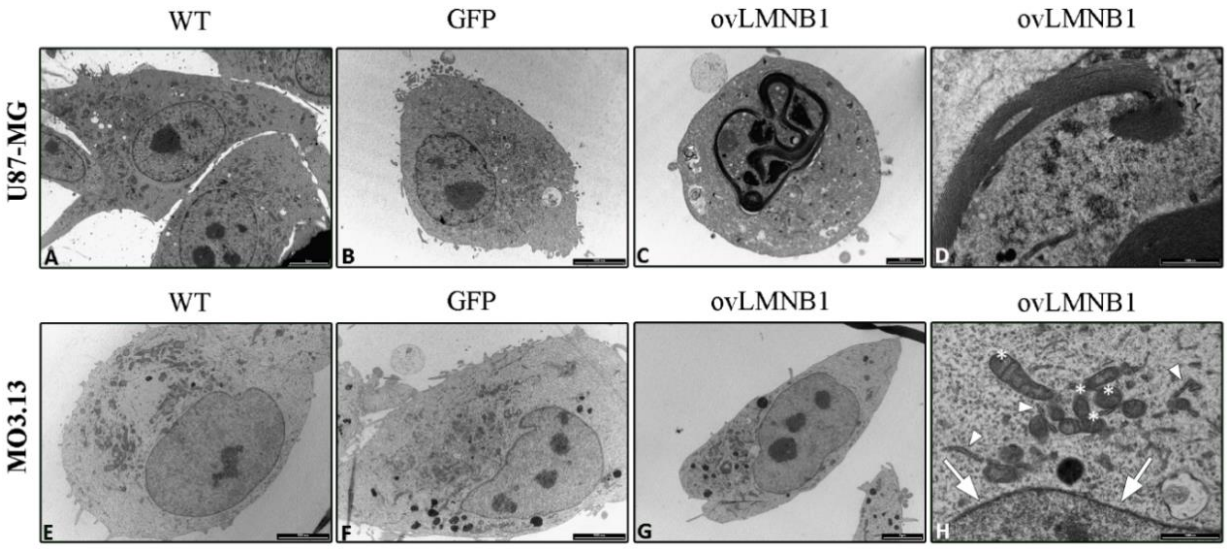

Figure 2 TEM analysis of U87-MG: (A) Wild type U87-MG cells observed at bar: 5 μm; (B) GFP transduced U87 cells at bar: 5000 nm; (C) U87-MG cells overexpressing Lamin B1 at bar: 2000 nm and (D) the nuclear envelope observed at bar: 1000 nm; TEM analysis of MO3.13 cells: (E) Wild type MO3.13 cells and (F) GFP transduced MO3.13 at bar: 5000nm;(G) MO3.13 cells overexpressing Lamin B1 at bar: 5 μm. (H) nuclear envelope(arrow), mitochondria (*) and regular endoplasmic reticulum (arrowhead) are visible at bar: 1000 nm. The results are representative of three independent experiments.

TEM analysis in U87-MG WT and GFP cells shows normal polygonal shape with round nuclei and well-preserved chromatin and nucleoli and a regular nuclear envelope composed by two membrane bilayers (**Fig. 2A and 2B**). In U87-MG cells overexpressing Lamin B1 (ovLMNB1) on the contrary a round-shaped morphology with misshaped and folded nuclei was observed (**Fig. 2C**) and at higher magnification, the nuclear envelope appears to be composed of stacked membrane layers surrounding the chromatin which is highly condensed in few masses (**Fig. 2D**).

MO3.13 WT and GFP cells show polygonal shape morphology, well-preserved nucleus, nucleoli and a normal nuclear envelope (**Fig. 2E and 2F**) and also MO3.13 overexpressing Lamin B1 shows well-preserved morphology, with regular shaped nuclei and nucleoli (**Fig. 2G**), and regular chromatin (**Fig. 2H**).

1.3. The overexpression of Lamin B1 causes both LIF and LIF-R reduction

Given the pivotal role that Leukemia Inhibitory Factor (LIF) has in the myelination and in the crosstalk between astrocytes and oligodendrocytes, it was examined the expression levels of LIF and its receptor LIF-R in U87-MG cells, the cells that produce LIF, and only the expression of LIF-R in MO3.13 cells, after Lamin B1 overexpression (**Fig. 3A-B**). Cells were tested after 48 hours of puromycin selection for total 96 hours of infection.

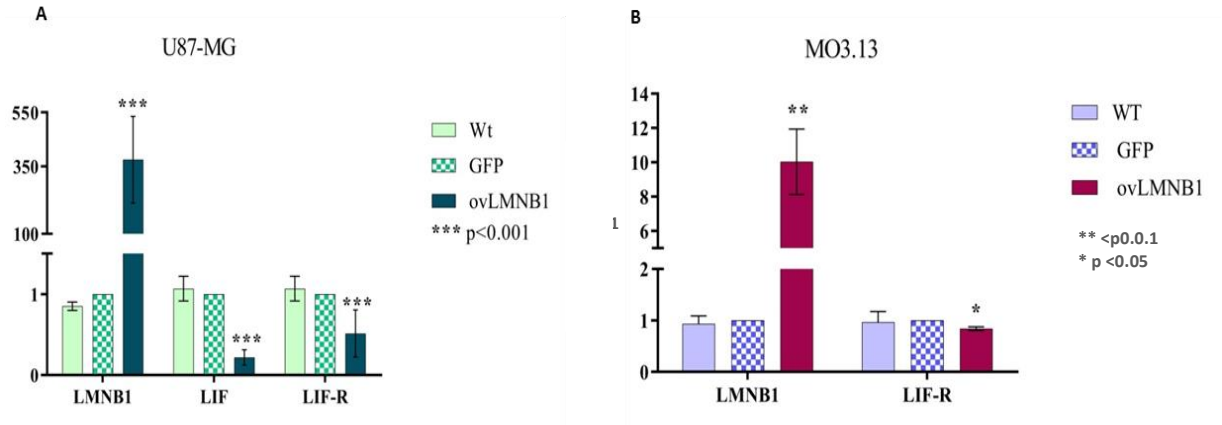

Figure 3 **(A-B)** qRT-PCR analysis shows that Lamin B1 overexpression reduces both LIF and LIF-R m RNA level in U87-MG (A) and LIF-R mRNA level in MO3.13 (B).

Real-time PCR analysis shows that in U87-MG cells overexpressing Lamin B1 there is a reduction of both LIF and LIF-R at mRNA levels compared to WT and GFP cells (**Fig. 3A**). In addition, also MO3.13 cells following Lamin B1 overexpression shows an important reduction of LIF-R expression (**Fig. B**). To confirm that LIF production was reduced in U87-MG cell overexpressing Lamin B1 Western blot analysis and ELISA test was performed (**Fig. 3C-D**).

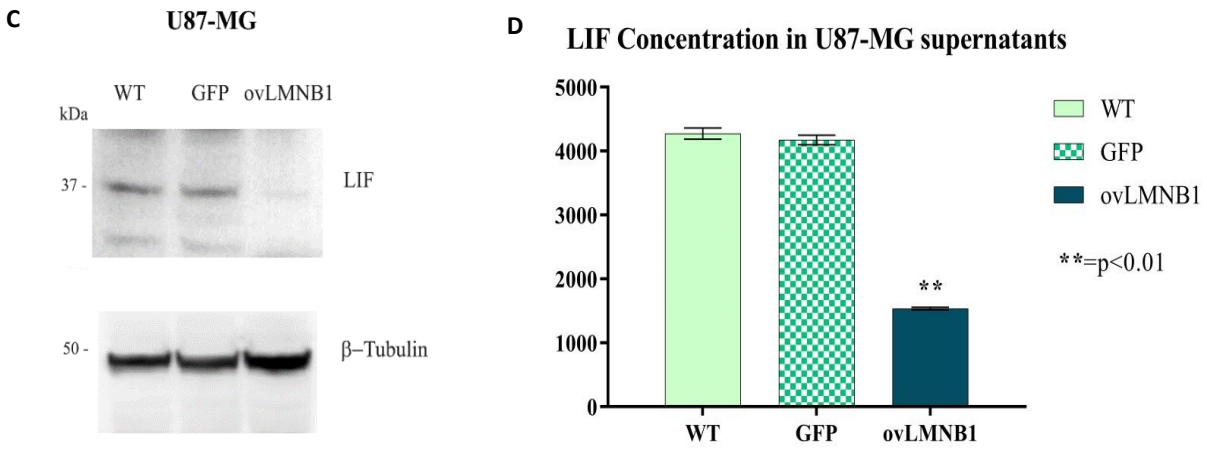

Figure3 **(C-D)** LIF protein expression in U87-MG analysed by western blot (C) and LIF concentration supernatants in U87-MG tested by ELISA test.

First, it was evaluated LIF production in WT, GFP and ovLMNB1 by Western blot, confirming the effective decrease in LIF expression following Lamin B1 overexpression (**Fig. 3C**). Next, we analysed LIF concentration in the supernatants of WT, GFP and ovLMNB1 by ELISA test demonstrating that LIF concentration was also in this case reduced in the supernatants of Lamin B1 overexpressing cells (**Fig. 3D**). This data suggests that the decrease seen at the

mRNA level corresponds to an actual decrease in LIF production at the protein level and in its release in the culture medium.

All the analyses are representative of three independent experiments, with *p<0.05; **p<0.01 and ***p<0.001 vs corresponding GFP sample. GAPDH and β-tubulin were used as housekeeping gene and loading control respectively.

1.4. Lamin B1 accumulation affects the LIF-R downstream pathways

To verify if the signalling cascades are active in Lamin B1 overexpressing cells when LIF binds to its receptor LIF-R, three principal pathways have been investigated: PI3K/AKT, Jak/STAT3 and ERK1/2 pathways. In particular, it was evaluated the expression and the phosphorylation of some fundamental molecules downstream LIF- signalling pathway in both U87-MG and MO3.13 cells 96 hours after transduction. Lamin B1 transduced cells (ovLMNB1) were compared to WT and GFP sample and β-tubulin was used as loading control for the expression or phosphorylation of several proteins (**Fig. 4**).

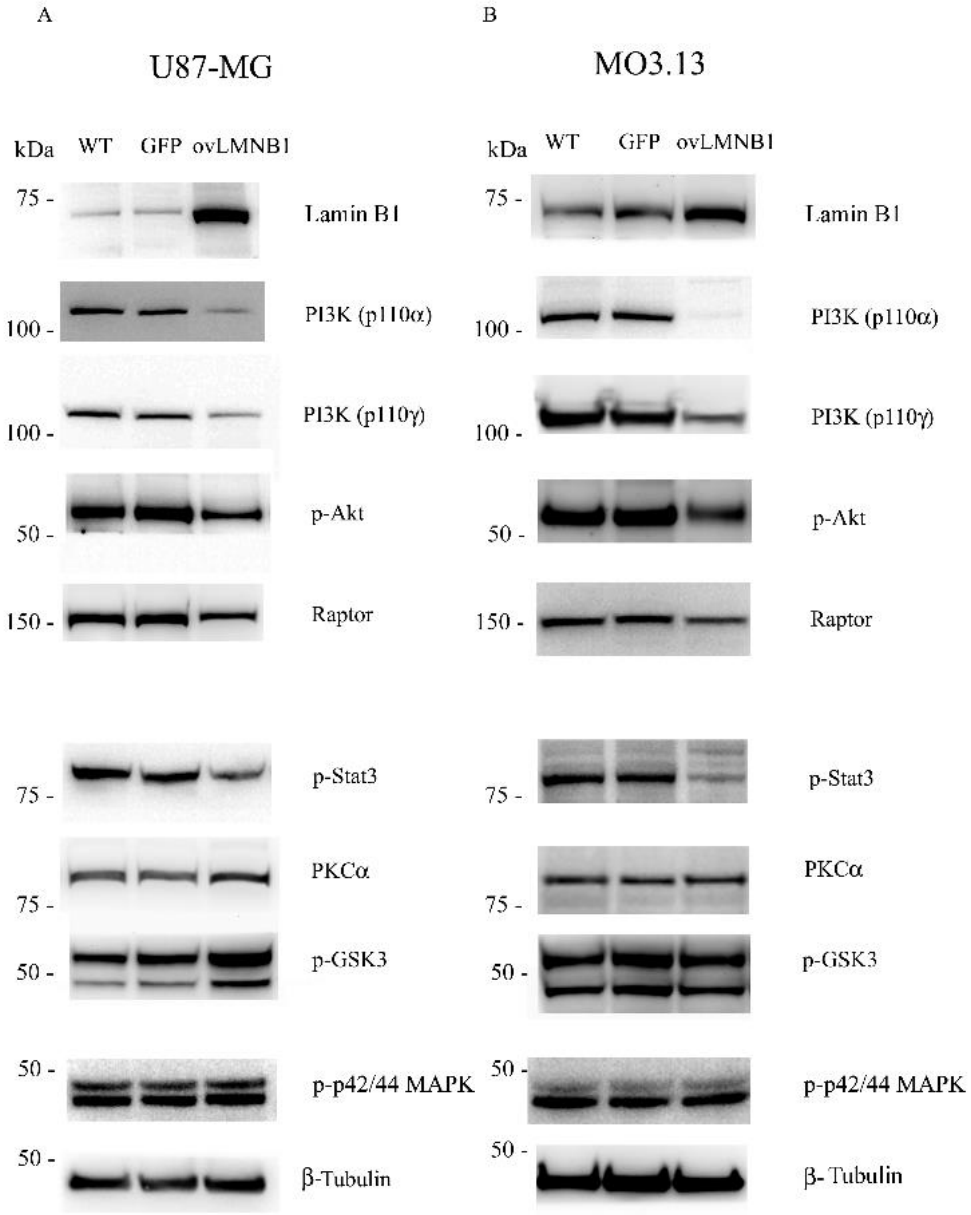

Figure 4 Effect of Lamin B1 accumulation on the expression and phosphorylation of LIF-R downstream signaling molecules. Analysis conducted by Western blot (A): representative panel for U87-MG and (B) for MO3.13.

Fig. 4A shows that Lamin B1 overexpression in U87-MG cells (ovLMNB1) leads to a down-regulation of the molecules belonging to the PI3K/AKT pathway. The amount of PI3K p110α and γ subunits were both reduced. Also, Akt phosphorylation and the expression of Raptor, the two components of mTORC1 complex, were reduced. However, the levels of phosphorylated GSK3 increased in parallel by the increase of PKCα expression. On the contrary, Stat3 pathway was downregulated, as confirmed by observing the reduction of

Stat3 phosphorylation compared to WT and GFP. Finally, the phosphorylation levels of p44/42 MAPK (Erk1/2) were not affected by Lamin B1 overexpression.

For what concerns MO3.13 cells, Lamin B1 overexpression also caused a reduction in PI3K activity as it can be seen through the reduction in PI3K p110α and γ expression, Akt phosphorylation and Raptor expression. Stat3 signalling was also downregulated but no alterations were observed in GSK3 phosphorylation, PKCα expression and Erk1/2 phosphorylation (**Fig. 4B**).

Western blot analyses are representative of three independent experiments.

1.5. Evaluation of LIF exogenous administration on the downregulated signalling pathways

In order to understand if LIF exogenous administration was able to revert the downregulated pathways downstream LIF-R after Lamin B1 overexpression, 48 hours after transduction and puromycin selection, U87-MG and MO3.13 cells were treated with LIF 80ng/ml for 48 hours. Then a Western blot analysis was performed to verify the activation of the downstream signalling pathways that in Lamin B1 overexpressing cells were altered. The expression or phosphorylation of the denoted molecules were analysed by using β-tubulin as loading control and comparing both U87-MG and MO3.13 overexpressing Lamin B1 with the respective WT and GFP control (**Fig.5**).

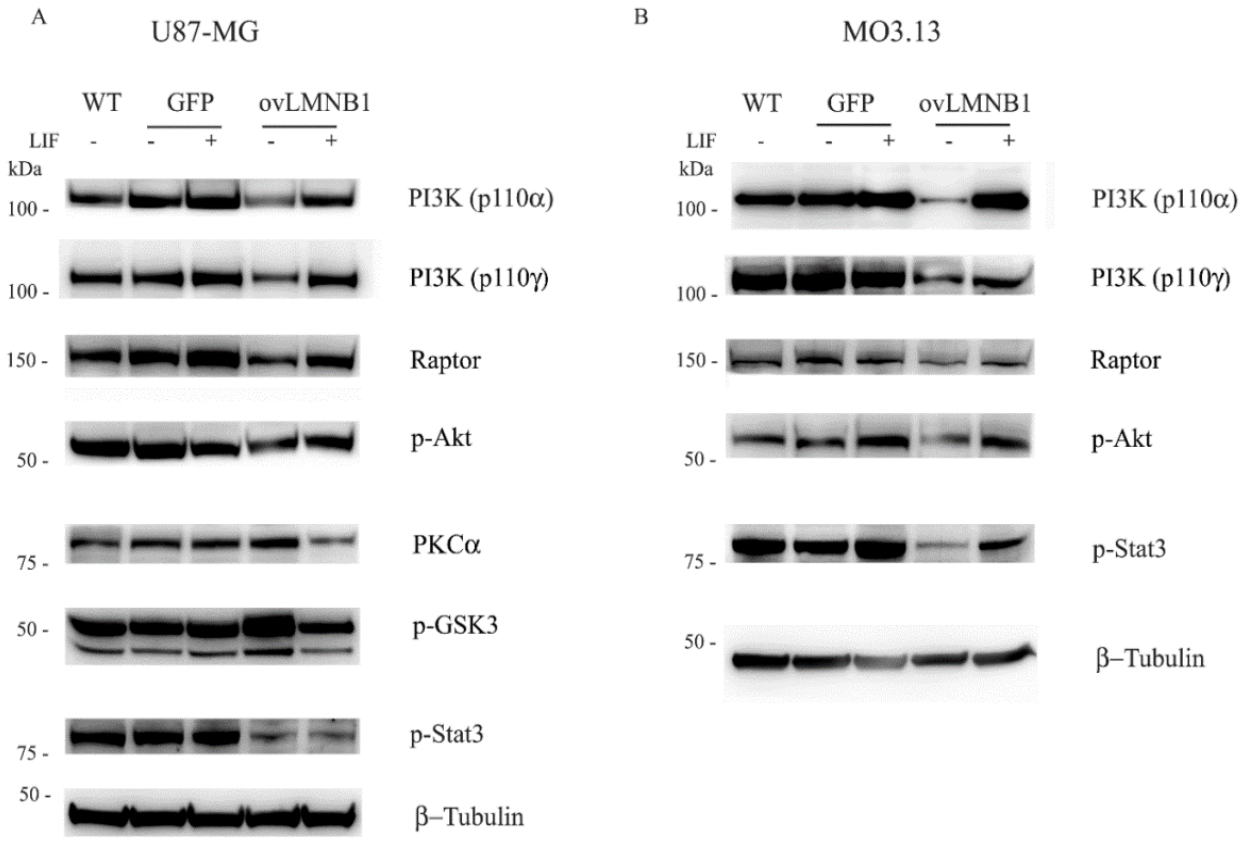

Figure 5 Effects of exogenous administration of on downregulated signaling pathways. Cells were transduced, puromycin-selected and either left in growth medium (-) or treated with LIF 80 ng/ml (+) for 48 hours. Panel (A) shows the effect in U87-MG and panel (B) in MO3.13.

Fig. 5A shows that in U87-MG cells, the administration of LIF to Lamin B1 overexpressing cells caused an increase of PI3K p110α and γ, Raptor expression and Akt phosphorylation. At the same time, it caused a reduction of PKCα expression and GSK3 phosphorylation but no effect was observed on Stat3 phosphorylation, which was lower in Lamin B1 overexpressing cells compared to WT and GFP cells also after LIF treatment.

For what concerns MO3.13 cells considering that they do not secrete LIF, it was tested also in this case if the stimulation with LIF could counteract the effects of Lamin B1 overexpression on the signalling pathways downstream LIF-R that are downregulated. Surprisingly in this case in Lamin B1 overexpressing cells LIF administration promotes not only an increase of PI3K p110α and γ, Raptor expression, and Akt phosphorylation, but also in Stat3 phosphorylation (**Fig. 5B**). These results are representative of three independent experiments, which demonstrated that exogenous administration of LIF on U87-MG could partially revert the effect of Lamin B1 overexpression on proteins belonging to the PI3K pathway but not reactivate Stat3 signalling. On the contrary, LIF administration on MO3.13 cells could reverse almost completely the effects of Lamin B1 overexpression that were associated to a reduction in LIF-R expression as is possible to see the increase of PI3K pathways and the re-activation of Stat3 phosphorylation.

Ex vivo model

2. Primary dermal fibroblasts of ADLD patients and controls

2.1. Lamin B1 duplication alters the nuclear structure of primary dermal fibroblasts

In primary dermal fibroblasts obtained from ADLD patients and healthy donors it was investigated firstly the expression of Lamin B1 at mRNA and protein levels and secondly their ultrastructure by TEM (**Fig 6A-B-C-D**).

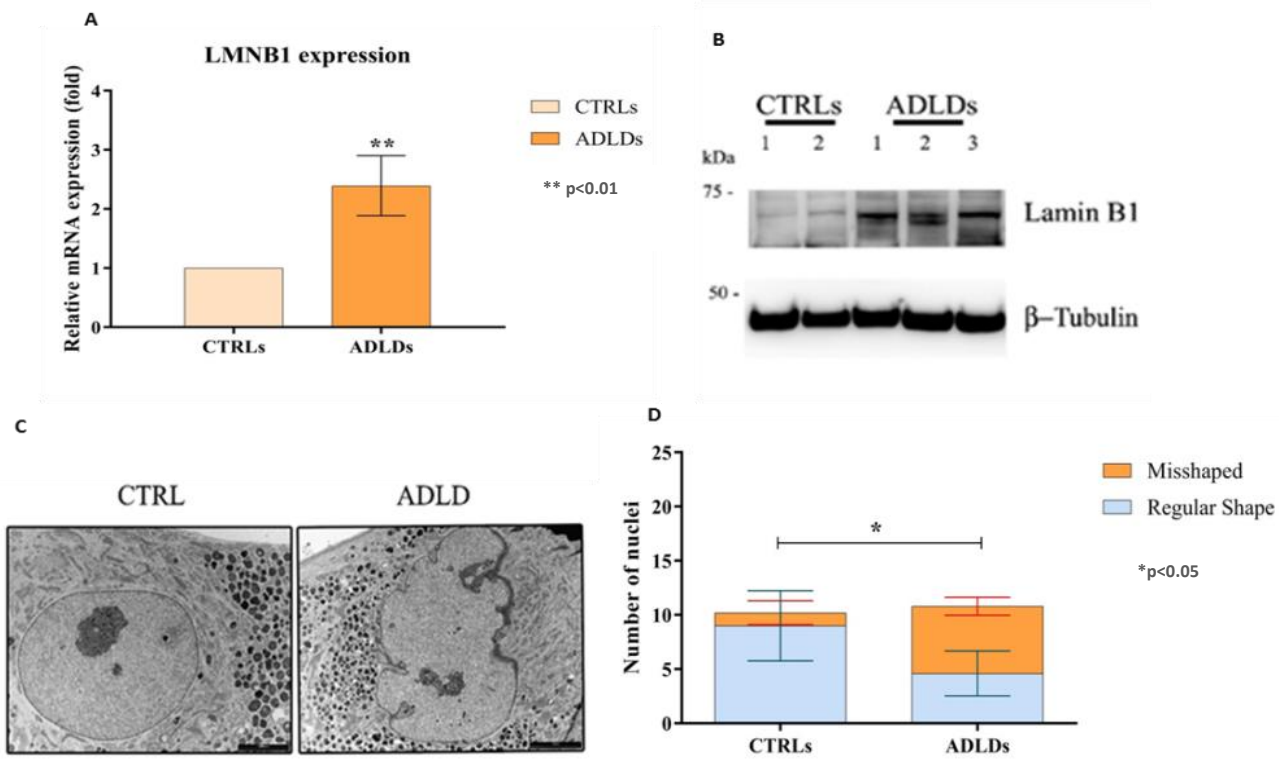

***Figure 6* (A-B-C-D)** Dermal primary fibroblasts from ADLD patients (ADLDs) and healthy donors (CTRLs) evaluated for Lamin B1 expression by qRT-PCR, data are expressed in percentage with ** p<0.01 vs control group (A). (B): Western blot evaluating Lamin B1 expression in healthy donors and ADLD patients. (C): Representative TEM analysis of dermal primary fibroblasts derived from healthy donors (CTRL) (bar: 5000nm) and ADLD patients (ADLD) (bar: 5 μm). (D): Quantitative analysis representing the number of misshaped nuclei compared to the number of regular nuclei observed in dermal primary fibroblasts from controls (n=6) and ADLD patients (n=6). Data are expressed in percentage with *p < 0.05.

Fig. 6A shows average mRNA expression levels for Lamin B1 in 6 ADLD patients and 6 healthy donors. Generally, fibroblasts from ADLD patients show elevated level of Lamin B1 mRNA expression compared to healthy donors but with high variability between samples of different patients. In fact, by observing the Western blot analysis (**Fig. 6B**) it is possible to notice that although ADLDs patients have a greater quantity of protein than the CTRLs, between them there is an evident variability. Anyway, analysing the ultrastructure by TEM, ADLD patients show more irregular and misshaped nuclei compared to CTRLs as shown in the **Fig. 6C** representative image of 6 primary dermal fibroblasts deriving from ADLD patients and 6 healthy donors analysed. **Fig. 6D** shows a quantitative analysis of the number of regular nuclei compared to misshaped nuclei observed in 6 control and 6 ADLD primary dermal fibroblasts. It displays the presence of 48.03% of misshaped nuclei in ADLD patients compared to 28.6% in healthy donors. Data are expressed in percentage with *$p<0.05$.

In order to verify whether the observations perceived in the primary cultures could be reproducible and related to the engineered model, dermal fibroblasts from one healthy donor were transduced with an empty vector (GFP) and a vector coding for the Lamin B1 (ovLMNB1). Lamin B1 expression was evaluated by real-time PCR and Western blot analysis. GAPDH and β-tubulin were used as loading control and both real-time PCR and Western blot is representative of three independent experiments (**Fig. 6E-F**).

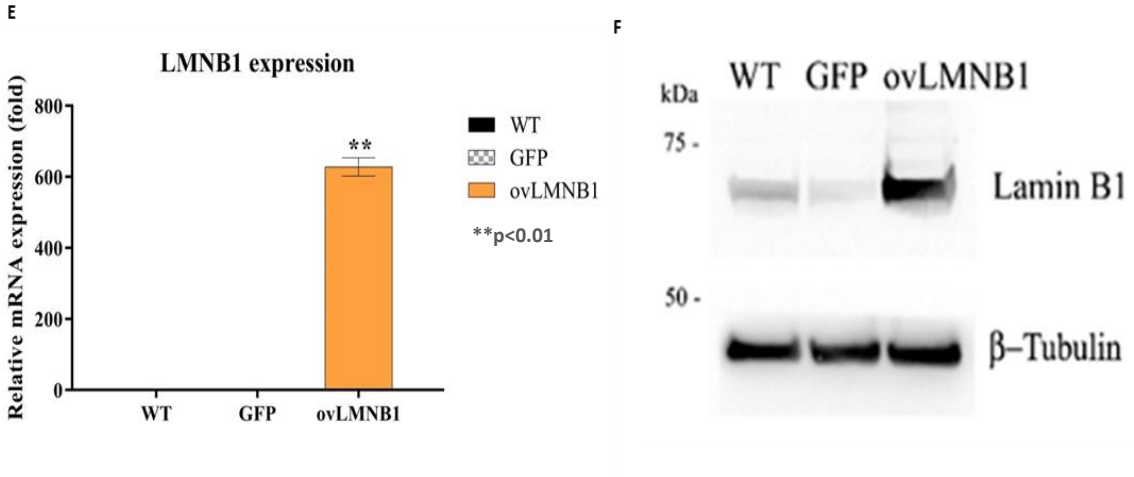

***Figure 6* (E-F)** Primary Dermal fibroblasts cultured from one healthy donor transduced with Lamin B1. (E): Lamin B1 mRNA level evaluated by qRT-PCR. (F): Lamin B1 protein expression by western blot analysis.

Following the assessment of Lamin B1 overexpression by real-time PCR and western blot, nuclear morphology was observed by TEM analysis (**Fig. 6G-H-I**) revealing that fibroblasts overexpressing Lamin B1 (**Fig. 6I**) showed misshaped and irregular nuclei respect to GFP (**Fig. 6H**) and control dermal fibroblast (**Fig. 6G**). On the contrary, the nuclear envelope of dermal fibroblasts overexpressing Lamin B1 did not show any stacked lamellar membranes.

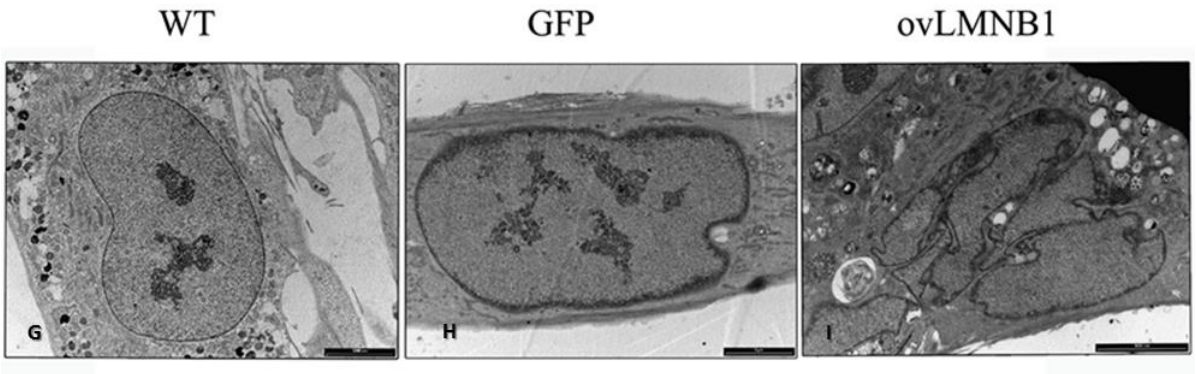

***Figure6* (G-H-I)** Ultrastructure of wild type, and empty vector and Lamin B1- transduced fibroblasts evaluated by TEM. Representative TEM images of (WT) and (GFP) observed at bar: 5000 nm and 1 μm, respectively; fibroblasts overexpressing Lamin B1 (ovLMNB1) observed at bar: 5000 nm.

2.2. Lamin B1 accumulation cause phosphorylation of inflammation mediators

Considering that fibroblasts are involved in chronic inflammation, it was controlled whether sample from ADLD patients and healthy donors differ in the activation of inflammation mediators. For this reason, following transduction of primary dermal fibroblasts from one healthy donor with empty vector GFP and Lamin B1 coding vector, , it was evaluated the phosphorylation level of NF-kB and STAT4 and compared to WT cells (**Fig 7A**). Then the correlation between Lamin B1 accumulation and NF-kB and STAT4 phosphorylation was also assessed in primary dermal fibroblasts derived from ADLD patients and healthy donors (**Fig 7B**).

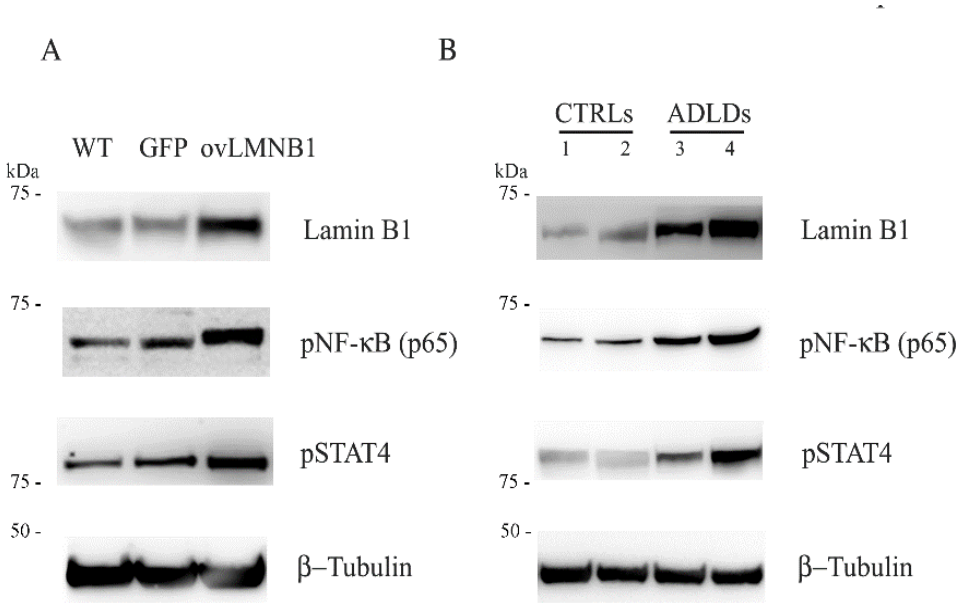

Figure7 **(A-B)** Lamin B1 overexpression and inflammation mediators. Primary dermal fibroblasts from one healthy donor, transduced with empty vector (GFP) and Lamin B1 (ovLMNB1) evaluated for NF-kB and STAT4 phosphorylation and compared to wild type cells (WT) (A). (B): Representative western blot showing NF-kB and STAT4 phosphorylation in fibroblasts from healthy donors (CTRLs) and ADLD patients (ADLDs).

Fig. 7A shows that following Lamin B1 overexpression, transduced fibroblasts (ovLMNB1) have higher levels of NF-kB S536 and STAT4 Y693 phosphorylation compared to GFP and WT sample. In the same way, **Fig. 7B** shows that the amount of phosphorylated NF-kB and Stat4 was higher in patients' fibroblasts compared to controls. Analysing statistically the densitometry values of the Western blot bands, significant difference in the phosphorylation levels between the two groups were compared (**Fig. 7C**) suggesting that ADLD patients present higher activation of inflammation pathways compared to healthy donors.

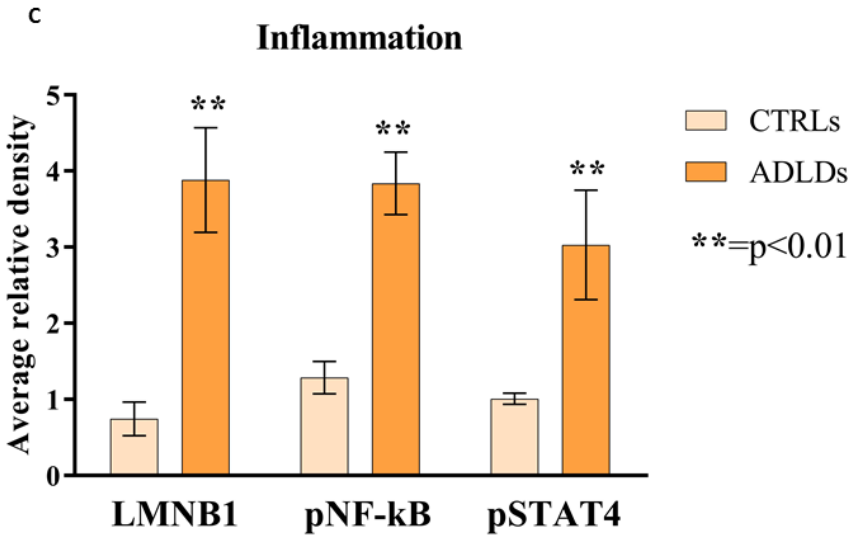

***Figure 7* (C)** Quantitative analysis of Lamin B1 expression, NF-kB and STAT4 phosphorylation in fibroblasts derived from 6 healthy donors and 6 ADLD patients.

In the Western blot analysis, β-tubulin was used as loading control (**A and B**). The quantitative analysis (**C**) was performed on 6 ADLD patients (ADLDs) and 6 healthy donors (CTRLs), and data are expressed as average ± SD, ** indicates $p<0.01$ vs control group.

2.3. In response to H_2O_2 treatment ADLD patients produce more ROS compared to healthy donors

Finally, it was evaluated another phenomena related to Lamin B1 expression, namely the production of reactive oxygen species (ROS) in response to H_2O_2 treatment. In order to determine if fibroblasts from ADLD patients and healthy donors are more responsive to oxidative stress, it was analysed the intracellular ROS production after 7 hours of H_2O_2 treatment in intervals of 15 minutes (**Fig 8**).

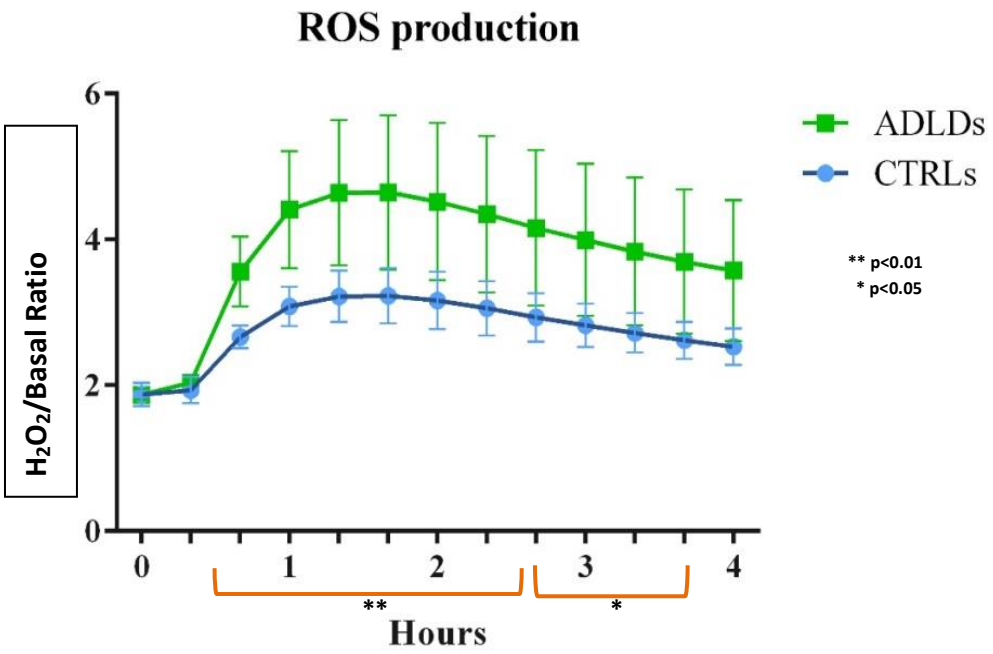

Figure 8 Fibroblasts' ROS production in response to H2O2 treatment evaluated in 6 healthy donors (CTRLs) and in 6 ADLD patients (ADLDs) every 15 minutes for 7 hours.

This graph shows the ratio between H_2O_2 induced and basal ROS production during the time course. After 45 minutes of stimulation, the production of ROS is higher in patients' fibroblasts compared to controls, although there is an increase in both (Fig. 8). The

difference between the mean values was statistically significant in the interval between 45 and 210 minutes after treatment, being highly significant between 60 and 135 minutes. The graph is the mean of three different experiments and the significance expressed with ** $p<0.01$ and * $p<0.05$.

Discussion

Autosomal Dominant Leukodystrophy is a rare disease where a duplication of a Lamin B1 gene leads to the demyelination of the central nervous system in an unknown way such that no effective therapies exist to date.

Considering the pivotal role that astrocytes and oligodendrocytes have in the myelination process this work aimed to highlight in detail what happens following Lamin B1 overexpression in both cell types.

For this reason, after infecting two cell lines U87-MG (astrocytes) and MO3.13 (oligodendrocytes) with a lentiviral vector coding for Lamin B1, the first data were quite surprising. In fact, after only 96 hours of infection, the two cell lines showed their first different characteristics. At the molecular and protein level astrocytes were more affected by Lamin B1 accumulation than oligodendrocytes. Although oligodendrocytes also showed a good amount of Lamin B1 both at molecular and protein level, the levels of the expression were not comparable to those of astrocytes. In fact, astrocytes showed Lamin B1 expression level at least 40 times greater than MO3.13 expression level (*Fig.1*). The subsequent morphological analysis of the two cell lines confirmed what was seen in previous analyses, showing that although the two infected cell lines showed clear morphological alterations compared to the respective wild type and empty control vector, again U87-MG presented more massive alterations of the nuclear shape respect MO3.13 cells.

These completely new and unexpected results have paved the way for a new way of investigation in order to try to understand what was "blocked" in the communication between these two cell lines such as to cause a demyelination. So, after an accurate study

about cell pathways that promote myelin production, it was decided to analyse a key factor that drives these two cells to produce myelin, namely LIF.

LIF is produced by astrocytes and other than supporting their survival, it favours the maturation of oligodendrocytes making them capable of producing the proteins necessary for myelin [46].

What was found in our engineered model is that in astrocytes an accumulation of Lamin B1 induces a reduction in LIF and in LIF-R at molecular level causing a decrease in LIF production and its cellular release. Moreover, oligodendrocytes, which cannot physiologically product LIF, showed a reduction in LIF-R expression.

Accordingly, the signalling pathways downstream LIF-R were investigated in both cells lines overexpressing Lamin B1, confirming that JAK-STAT3 and PI3K/AKT axes are downregulated, while MAPK/ERK axis is not affected. These results may be explained by the fact that the first two pathways have a direct connection to LIF axis while MAPK/ERK pathway is connected to many other mediators. Additionally, it is very interesting to observe that in U87-MG cells overexpressing Lamin B1 GSK3 is more phosphorylated in combination with the increase of PKCα expression, suggesting a possible involvement of this protein in the GSK3 phosphorylation. In MO3.13 cells overexpressing Lamin B1 no variation in GSK3 phosphorylation was observed. Therefore, to confirm that the downregulation of the pathways implicated in cell survival were actually due to the overexpression of Lamin B1, which somehow blocks both LIF production and its receptor expression, we investigated whether exogenous LIF administration could recover the activation of the signalling pathways downstream LIF-R. It is important to highlight that also these experiments have shown differences between the two cell lines. In particular, the administration of LIF promotes a phenotype rescue for what concern the protein expression of PI3K p110 α and γ,

Raptor and Akt phosphorylation in both U87-MG and MO3.13 cells overexpressing Lamin B1. Instead, GSK3 phosphorylation and PKCα expression are reduced only in U87-MG cells overexpressing Lamin B1. Probably the treatment induces a reduction of PKCα expression, which consecutively reduces the phosphorylation of GSK3. Therefore, the re-activation both of PI3K axis and PKCα/ GSK3 may be involved in promoting cell survival. Moreover, LIF administration promotes the STAT3 phosphorylation, but only in MO3.13 cells overexpressing Lamin B1. This evidence underlies that it is possible to restore the activation of wild type pathways only in oligodendrocytes, using exogenous administration of LIF. This difference may be due to the fact that oligodendrocytes are less affected morphologically by Lamin B1 accumulation than astrocytes, resulting in their ability to take advance by LIF administration and bypass the downregulated receptor. In astrocytes, in which Lamin B1 accumulation causes the reduction of both LIF and LIF-R expression, LIF administration can only partially restore the signalling downstream LIF-R. In fact, STAT3 phosphorylation cannot be re-established highlighting that Lamin B1 overexpression drastically affects astrocytic function reducing the essential support for oligodendrocytes during the myelination process. This is the first time that the identification of cellular signalling and morphological alterations in astrocytes has been linked to the ADLD disease. In fact, until now, their role in the disease has only been presumed but never investigated.

Additionally, also primary dermal fibroblasts derived from ADLD patients and fibroblasts transduced to overexpress Lamin B1 have shown the ultrastructural nuclear alterations similar to those described in the engineer model, such as misshaped and folded nuclei, although with less marked evidence. Moreover, in order to add another piece of information to this intriguing rare disease we considered that LIF other than promoting astrocytes maturation, activation, and oligodendrocytes differentiation, is also considered a potential

therapeutic drug for Multiple sclerosis (MS) [69] and neuroinflammatory lesions [70]. Therefore, it was investigated the role of inflammation in ADLD primary dermal fibroblasts observing that ADLD primary fibroblasts have an increase in the phosphorylation of NF-kB and STAT4, two important inflammation mediators.

Finally, considering that oxidative stress has been linked to Lamin B1 accumulation [71] and age dependent alterations, it was also investigated the ROS production in response to H_2O_2 treatment comparing ADLD primary fibroblasts with the healthy donors, highlighting that ADLD primary fibroblasts produce more ROS than healthy donors .

Surely all these evidences are part of a vast series of evidences destined to intertwine and that is why further studies need to be carried out. However, highlighting that astrocyte dysfunction could represent the foundation of the disease opens the way to new possible paths of investigation in ADLD studies.

Conclusions and Future perspectives

As previously mentioned, this is the first time that morphological and cellular signalling alterations in astrocytes have been linked to the ADLD disease.

From the morphological point of view, our results have demonstrated that astrocytes cell line overexpressing Lamin B1, show severe ultrastructural nuclear alterations, such as misshaped and folded nuclei, like in ADLD patients' primary dermal fibroblasts, while the same alterations are not present in the oligodendrocytes cell line overexpressing Lamin B1.

This suggests that it is possible those different cellular types respond in different ways to the overexpression of Lamin B1 and that the accumulation of Lamin B1 in astrocytes might be pivotal in determining oligodendrocytes dysfunction via cellular signalling mechanisms. Indeed, our results have demonstrated that the communication between astrocytes and oligodendrocytes might be altered due to the reduction of LIF release and LIF-R downregulation, which are critical elements in the myelination process [46]. In addition, while considering the intrinsic model limitations in the investigation of the role of inflammation and oxidative stress in ADLD primary dermal fibroblasts, our results have highlighted an increase in both in ADLD patients' cells. These data suggest a possible correlation between lipid alterations, inflammation and stress age-related processes [72], which could be at the base of a negative loop mechanisms that leads to the progression of ADLD phenotype.

For all these reasons, future studies may be directed primarily towards the preparation of co-cultures of immortalized astrocytes and oligodendrocyte precursor cells (OPC), in order to better understand if the signalling and morphological alterations highlighted in the immortalized cell lines, can be confirmed in more physiological conditions. Co-culture might

be set up by inducing Lamin B1 overexpression in OPCs and putting them in culture with mature astrocytes, to determine OPCs' ability to differentiate and maturate in response to LIF secreted by astrocytes. The expression of the proteins MBP, PLP, MOG required for myelin winding could be evaluated. At the same time the complementary experiment could be performed, therefore inducing Lamin B1 overexpression in astrocytes and testing their ability to induce OPCs differentiation. Moreover, using advanced 3D imaging techniques, a co-culture of astrocytes, oligodendrocytes and neurons could be created in order to observe the effective myelination/demyelination process directly on the axons, following the overexpression of Lamin B1 in both astrocytes and oligodendrocytes or in one cell type at the time. These aspects will be essential for the confirmation of the proposed pathological mechanisms.

Then, considering the correlation between morphological alteration and Lamin B1 accumulation, and the aberrant expression of lipids evident in various neurological disorders [73], the alteration of lipid signalling pathways might represent an important event underlying the disease phenotype. For these reasons and considering that lipids play active roles in myelination process, one might investigate the possible alteration of lipid pathways and whereas phosphoinositide dependent phospholipases (PI-PLCs) may be altered in the pathological phenotype. Indeed these molecules are very abundant in the brain (especially the isoforms PI-PLCβ1, PI-PLCɣ1 and PI-PLCβ4) and can be involved in several lipid signalling pathway alterations [74] .

Finally, thanks to the collaboration between the Cellular Signalling Laboratory and the Korean Brain Research Institute (KBRI), iPSCs (induced pluripotent stem cells) from ADLD primary fibroblasts could be induced to differentiate towards a glial phenotype in order to study the molecular and morphological changes on patients' primary cells.

In conclusion, if the results of our *in vitro* model, which highlight for the first time the astrocyte as a determinant player in establishing ADLD phenotype, will be reproducible in the future experiments mentioned above, undoubtedly it will be a new starting point for future investigations. In fact, it will be possible to create new animal models with the overexpression of Lamin B1 in astrocytes, thus abandoning the unsuccessful previous models. Moreover, the identification of signal transduction pathways alterations that regulate the myelination process of glial cells, will help to identify the underlying mechanisms that lead to the onset of the pathological phenotype and to discover molecular therapies increasingly targeted and safer.

References

1. Padiath, Q. S. *et al.* Lamin B1 duplications cause autosomal dominant leukodystrophy. *Nat. Genet.* **38**, 1114–1123 (2006).

2. Philips, T. *et al.* Oligodendroglia: Metabolic supporters of neurons. *Journal of Clinical Investigation* vol. 127 3271–3280 (2017).

3. Kıray, H. *et al.* The multifaceted role of astrocytes in regulating myelination. *Exp. Neurol.* **283**, 541–549 (2016).

4. Lin, S. T. *et al.* Regulation of myelination in the central nervous system by nuclear lamin B1 and Non-coding RNAs. *Transl. Neurodegener.* **3**, 1–8 (2014).

5. Mosser, J. *et al.* Putative X-linked adrenoleukodystrophy gene shares unexpected homology with ABC transporters. *Nature* **361**, 726–730 (1993).

6. Engelen, M. *et al.* X-linked adrenoleukodystrophy (X-ALD): Clinical presentation and guidelines for diagnosis, follow-up and management. *Orphanet Journal of Rare Diseases* vol. 7 51 (2012).

7. Helman, G. *et al.* Disease specific therapies in leukodystrophies and leukoencephalopathies. *Molecular Genetics and Metabolism* vol. 114 527–536 (2015).

8. Appikatla, S. *et al.* Insertion of proteolipid protein into oligodendrocyte mitochondria regulates extracellular pH and adenosine triphosphate. *Glia* **62**, 356–373 (2014).

9. Eldridge, R. *et al.* Hereditary Adult-Onset Leukodystrophy Simulating Chronic Progressive Multiple Sclerosis. *N. Engl. J. Med.* **311**, 948–953 (1984).

10. Schwankhaus, J. D. *et al.* Clinical and pathological features of an autosomal dominant, adult-onset leukodystrophy simulating chronic progressive multiple sclerosis. *Arch. Neurol.* **51**, 757–766 (1994).

11. Eldridge R. *et al.* Hereditary adult-onset leukodystrophy simulating chronic progressive multiple sclerosis. *New Engl. J. Med.* **311**, 948–53 (1984).

12. Quattrocolo G. *et al.* Autosomal dominant late-onset leukoencephalopathy:clinical

report of a new Italian family. *Eur Neurol* **37**, 53–61 (1997).

13. Brussino, A. *et al.* A novel family with Lamin B1 duplication associated with adult-onset leucoencephalopathy. *J. Neurol. Neurosurg. Psychiatry* **80**, 237–240 (2009).

14. Marklund, L. *et al.* Adult-onset autosomal dominant leukodystrophy with autonomic symptoms restricted to 1.5 Mbp on chromosome 5q23. *Am. J. Med. Genet. Part B Neuropsychiatr. Genet.* **141**, 608–614 (2006).

15. Meijer, I. A. *et al.* A novel duplication confirms the involvement of 5q23.2 in autosomal dominant leukodystrophy. *Arch. Neurol.* **65**, 1496–1501 (2008).

16. Schuster, J. *et al.* Genomic duplications mediate overexpression of lamin B1 in adult-onset autosomal dominant leukodystrophy (ADLD) with autonomic symptoms. *Neurogenetics* **12**, 65–72 (2011).

17. Dos Santos, M. M. *et al.* Adult-onset autosomal dominant leukodystrophy due to LMNB1 gene duplication. *J. Neurol.* **259**, 579–581 (2012).

18. Potic, A. *et al.* Adult-onset autosomal dominant leukodystrophy without early autonomic dysfunctions linked to lamin B1 duplication: A phenotypic variant. *J. Neurol.* **260**, 2124–2129 (2013).

19. Coffeen, C. M. Genetic localization of an autosomal dominant leukodystrophy mimicking chronic progressive multiple sclerosis to chromosome 5q31. *Hum. Mol. Genet.* **9**, 787–793 (2000).

20. Giorgio, E. *et al.* Analysis of LMNB1 duplications in autosomal dominant leukodystrophy provides insights into duplication mechanisms and allele-specific expression. *Hum. Mutat.* **34**, 1160–1171 (2013).

21. Brussino, A. *et al.* A family with autosomal dominant leukodystrophy linked to 5q23.2-q23.3 without lamin B1 mutations. *Eur. J. Neurol.* **17**, 541–549 (2010).

22. Padiath, Q. S. *et al.* *Autosomal Dominant Leukodystrophy Caused by Lamin B1 Duplications. A Clinical and Molecular Case Study of Altered Nuclear Function and Disease*. *Methods in Cell Biology* vol. 98 (Elsevier Masson SAS, 2010).

23. Asahara, H. *et al.* A Japanese family with probably autosomal dominant adult-onset

leukodystrophy. *Rinsho Shinkeigaku* **36**, 968–972 (1996).

24. Labauge, P. *et al.* Dominant form of vanishing white matter-like leukoencephalopathy. *Ann. Neurol.* **58**, 634–639 (2005).

25. Costello, D. J. *et al.* Leukodystrophies classification, diagnosis, and treatment. *Neurologist* vol. 15 319–328 (2009).

26. Padiath, Q. S. Autosomal Dominant Leukodystrophy: A disease of the nuclear lamina. *Front. Cell Dev. Biol.* **7**, 1–6 (2019).

27. Melberg, A. *et al.* MR characteristics and neuropathology in adult-onset autosomal dominant leukodystrophy with autonomic symptoms. *Am. J. Neuroradiol.* **27**, 904–911 (2006).

28. Aebi, U. *et al.* The nuclear lamina is a meshwork of intermediate-type filaments. *Nature* **323**, 560–564 (1986).

29. Lin, F. & Worman, H. J. Structural organization of the human gene encoding nuclear lamin A and nuclear lamin C. *J. Biol. Chem.* **268**, 16321–16326 (1993).

30. Gerace, L. & Burke, B. Functional organization of the nuclear envelope. *Annual Review of Cell Biology* vol. 4 335–374 (1988).

31. Lin, F. & Worman, H. J. Structural organization of the human gene (LMNB1) encoding nuclear lamin B1. *Genomics* vol. 27 230–236 (1995).

32. Stuurman, N. *et al.* Nuclear lamins: Their structure, assembly, and interactions. *J. Struct. Biol.* **122**, 42–66 (1998).

33. Goldman, R. D. *et al.* Nuclear lamins: Building blocks of nuclear architecture. *Genes and Development* vol. 16 533–547 (2002).

34. Parnaik, V. K. Role of Nuclear Lamins in Nuclear Organization, Cellular Signaling, and Inherited Diseases. *Int. Rev. Cell Mol. Biol.* **266**, 157–206 (2008).

35. Maraldi, N. M. *et al.* Laminopathies and lamin-associated signaling pathways. *J. Cell. Biochem.* **112**, 979–992 (2011).

36. Malhas, A. N. *et al.* Lamin B1 controls oxidative stress responses via Oct-1. *J. Cell Biol.* **184**, 45–55 (2009).

37. Ferrera, D. *et al.* Lamin B1 overexpression increases nuclear rigidity in autosomal dominant leukodystrophy fibroblasts. *FASEB J.* **28**, 3906–3918 (2014).

38. Columbaro, M. *et al.* Oct-1 recruitment to the nuclear envelope in adult-onset autosomal dominant leukodystrophy. *Biochim. Biophys. Acta - Mol. Basis Dis.* **1832**, 411–420 (2013).

39. Barascu, A. *et al.* Oxidative stress induces an ATM-independent senescence pathway through p38 MAPK-mediated lamin B1 accumulation. *EMBO J.* **31**, 1080–1094 (2012).

40. Dreesen, O. *et al.* Lamin B1 fluctuations have differential effects on cellular proliferation and senescence. *J. Cell Biol.* **200**, 605–17 (2013).

41. Dreesen, O. *et al.* The contrasting roles of lamin B1 in cellular aging and human disease. *Nucleus* **4**, 283–290 (2013).

42. Wang, A. S. *et al.* Loss of lamin B1 is a biomarker to quantify cellular senescence in photoaged skin. *Sci. Rep.* **7**, (2017).

43. Chojnowski, A. *et al.* Nuclear lamina remodelling and its implications for human disease. *Cell Tissue Res.* **360**, 621–31 (2015).

44. Costello, D. J. *et al.* Leukodystrophies classification, diagnosis, and treatment. *Neurologist* vol. 15 319–328 (2009).

45. Lyon, G. *et al.* Leukodystrophies: Clinical and genetic aspects. *Topics in Magnetic Resonance Imaging* vol. 17 219–242 (2006).

46. Ishibashi, T. *et al.* Astrocytes promote myelination in response to electrical impulses. *Neuron* **49**, 823–832 (2006).

47. Dupree, J. L. *et al.* Olirdendrocytes assist in the maintenance of sodium channel clusters independent of the myelin sheath. *Neuron Glia Biol.* **1**, 179–192 (2004).

48. Philips, T. & Rothstein, J. D. R E V I E W S E R I E S : G L I A A N D N E U R O D E G E N E R AT I O N Series Editors: Marco Colonna and David Holtzmann. *J. Clin. Invest.* **127**, 3271–3280 (2017).

49. Stadelmann, C. *et al.* Myelin in the central nervous system: Structure, function, and pathology. *Physiol. Rev.* **99**, 1381–1431 (2019).

50. Sherman, D. L. & Brophy, P. J. Mechanisms of axon ensheathment and myelin growth. *Nat. Rev. Neurosci.* **6**, 683–690 (2005).

51. Barres, B. A. The Mystery and Magic of Glia: A Perspective on Their Roles in Health and Disease. *Neuron* **60**, 430–440 (2008).

52. Gearing, D. P. *et al.* Molecular cloning and expression of cDNA encoding a murine myeloid leukaemia inhibitory factor (LIF). *EMBO J.* **6**, 3995–4002 (1987).

53. Yue, X. *et al.* The Regulation of Leukemia Inhibitory Factor. *Cancer Cell Microenviron.* **2**, (2015).

54. Moon, C. *et al.* Leukemia inhibitory factor inhibits neuronal terminal differentiation through STAT3 activation. *Proc. Natl. Acad. Sci. U. S. A.* **99**, 9015–9020 (2002).

55. Hendriks, J. J. A. *et al.* Leukemia inhibitory factor modulates production of inflammatory mediators and myelin phagocytosis by macrophages. *J. Neuroimmunol.* **204**, 52–57 (2008).

56. Suzuki, S. *et al.* Activation of cytokine signaling through leukemia inhibitory factor receptor (LIFR)/gp130 attenuates ischemic brain injury in rats. *J. Cereb. Blood Flow Metab.* **25**, 685–693 (2005).

57. Davis, S. M. & Pennypacker, K. R. The role of the leukemia inhibitory factor receptor in neuroprotective signaling. *Pharmacology and Therapeutics* vol. 183 50–57 (2018).

58. Haroon, F. *et al.* Gp130-Dependent Astrocytic Survival Is Critical for the Control of Autoimmune Central Nervous System Inflammation. *J. Immunol.* **186**, 6521–6531 (2011).

59. Gaudet, A. D. & Fonken, L. K. Glial Cells Shape Pathology and Repair After Spinal Cord Injury. *Neurotherapeutics* vol. 15 554–577 (2018).

60. Lin, S. T. & Fu, Y. H. miR-23 regulation of lamin B1 is crucial for oligodendrocyte development and myelination. *DMM Dis. Model. Mech.* **2**, 178–188 (2009).

61. Lo Martire, V. *et al.* Mice overexpressing lamin B1 in oligodendrocytes recapitulate the age-dependent motor signs, but not the early autonomic cardiovascular dysfunction of autosomal-dominant leukodystrophy (ADLD). *Exp. Neurol.* **301**, 1–12

(2018).

62. Rolyan, H. *et al.* Defects of lipid synthesis are linked to the age-dependent demyelination caused by Lamin B1 overexpression. *J. Neurosci.* **35**, 2002–12017 (2015).

63. Heng, M. Y. *et al.* Lamin B1 mediates cell-autonomous neuropathology in a leukodystrophy mouse model. *J. Clin. Invest.* **123**, 2719–2729 (2013).

64. Yattah, C. *et al.* Dynamic Lamin B1-Gene Association During Oligodendrocyte Progenitor Differentiation. *Neurochem. Res.* **45**, 606–619 (2020).

65. Giorgio, E. *et al.* Allele-specific silencing as treatment for gene duplication disorders: Proof-of-principle in autosomal dominant leukodystrophy. *Brain* **142**, 1905–1920 (2019).

66. Rolyan, H. *et al.* Defects of lipid synthesis are linked to the age-dependent demyelination caused by Lamin B1 overexpression. *J. Neurosci.* **35**, 2002–12017 (2015).

67. Camps, J. *et al.* The role of lamin Bl for the maintenance of nuclear structure and function. *Nucleus* **6**, 8–14 (2015).

68. Fukuda, S. *et al.* Negative regulatory effect of an oligodendrocytic bHLH factor OLIG2 on the astrocytic differentiation pathway. *Cell Death Differ.* **11**, 196–202 (2004).

69. Rittchen, S. *et al.* Myelin repair invivo is increased by targeting oligodendrocyte precursor cells with nanoparticles encapsulating leukaemia inhibitory factor (LIF). *Biomaterials* **56**, 78–85 (2015).

70. Roe, C. Unwrapping Neurotrophic Cytokines and Histone Modification. *Cell. Mol. Neurobiol.* **37**, (2017).

71. Shimi, T. & Goldman, R. D. Nuclear lamins and oxidative stress in cell proliferation and longevity. *Adv. Exp. Med. Biol.* **773**, 415–430 (2014).

72. Padiath, Q. S. Lamin B1 mediated demyelination: Linking Lamins, Lipids and Leukodystrophies. *Nucleus* **7**, 547–553 (2016).

73. Ratti, S. *et al.* Nuclear Inositide Signaling Via Phospholipase C. *J. Cell. Biochem.* **118**,

1969–1978 (2017).

74. Ratti, S. *et al.* Nuclear phospholipase C isoenzyme imbalance leads to pathologies in brain, hematologic, neuromuscular, and fertility disorders. *J. Lipid Res.* **60**, 312–317 (2019).